Fall 2023

Exploring forest structural complexity: scale effects and metric relationships in New England hardwood forests

Alex Jed Siebert
University of New Hampshire

Exploring forest structural complexity: scale effects and metric relationships in New England hardwood forests

By

Jed Siebert

B.A. Earth and Environmental Science, Wesleyan University, 2016

THESIS

Submitted to the University New Hampshire in Partial Fulfillment of the Requirements for the Degree of

Master of Science

in

Forestry

September, 2023

This Thesis has been examined and approved in partial fulfillment of the requirements for the degree of Master of Science in Forestry by:

Thesis Director, Dr. Mark Ducey, Chair, Department of Natural Resources and the Environment

Dr. Olivia Fraser, Analyst, USDA Forest Service

Dr. John Gunn, Affiliate Faculty, Department of Natural Resources and the Environment

On July 20, 2023

Approval signatures are on file with the University of New Hampshire Graduate School.

ACKNOWLEDGEMENTS

Completing this work would not have been possible without the guidance and encouragement I have received throughout the process from many individuals.

First, I would like to express my sincerest gratitude to my advisor, Dr. Mark Ducey. His mentorship, expertise, and encouragement have been instrumental in this research.

I would like to thank Dr. Olivia Fraser and Dr. John Gunn for serving on my thesis committee and providing valuable insights and constructive feedback.

I would like to thank all field crew members who have helped collect data, including Rosa Bailey, Jenna Farrell, Jay Parry, Sally Pizzuto, and Natalie Unger-Mochrie.

Finally, I would like to extend my deepest gratitude to all my friends and loved ones for their endless support.

TABLE OF CONTENTS

LIST OF FIGURES

LIST OF TABLES

ABSTRACT

Forest structural complexity (FSC) is an informative characteristic in forest management due to its connections to ecosystem resilience, biodiversity, and carbon sequestration. Despite its widespread use, quantifying FSC remains a challenge because of the many attributes that can comprise an assessment of FSC and ambiguity around what exactly is meant by "complexity." Many assessments of FSC involve metrics derived from lidar data, yet there is not a clear understanding of how spatial extent impacts metrics of FSC. This thesis investigates the influence of spatial extent on FSC metrics and metric relationships in the context of New England mixed hardwood forests.

Chapter 1 examines the role of spatial extent in FSC metrics. Analysis of correlations between FSC metrics across a range of plot sizes revealed relationships that suggest smaller plot sizes, with a radius of 10 meters or smaller, can be adequately representative of larger areas. This observation has implications for lidar data processing efficiency and cost-effectiveness.

Chapter 2 explores the relationships between field-derived and lidar-derived metrics of FSC. Some noteworthy patterns emerged, emphasizing the significance of several classes of FSC characteristics, including size-related and canopy-related variables. The alignment of field-based and lidar-derived metrics underscores their complementarity in characterizing forest structure.

This research elucidates some of the intricacies of quantifying FSC and identifies categories for comprehensive assessments of FSC, using canopy height, height diversity, canopy cover,

outer canopy complexity, and diameter diversity. This should provide a useful framework for future studies involving FSC assessments.

CHAPTER 1: The scale-dependency of lidar-derived metrics of forest structural complexity

1.1 Introduction

Assessing the diversity of an ecosystem is a complex matter. While the term "biodiversity" is a relatively recent invention (Sarkar, 2002), concepts and measurements of diversity in ecology have existed for the better part of a century (Sarkar, 2002; Simpson, 1949; Takacs, 1996; Whittaker, 1972). Ecosystems can be characterized in a variety of ways, but frequently, researchers will describe ecosystems according to their species composition rather than their ecological processes like disturbance and nutrient cycling (Magurran, 1988; Noss, 1990). While compositional diversity is meaningful, it does not necessarily characterize an ecosystem holistically (McElhinny et al., 2005). To address this shortfall, researchers have also suggested describing characteristics that pertain to the function and structure of an ecosystem (Franklin et al., 1981, 2002; Noss, 1990).

Understanding forest structure is critical to sustainable forest management. In essence, forest structure is the spatial arrangement of trees, alive and dead, and their components relative to one another and the non-living components of the space they inhabit. By examining the structure of a forest, researchers can gain insights into the processes that control forest dynamics and, importantly, use findings to inform management decisions (McElhinny et al., 2005).

Research on forest structure and ecosystem function has reinforced the importance of forest structural complexity (FSC) (Hardiman et al., 2011, 2013; E. LaRue et al., 2019; Thom & Keeton, 2019). Furthermore, the growing knowledge of FSC has led to an increasing

emphasis on creating structurally complex forest stands to promote ecosystem resilience, ecosystem function, productivity, carbon storage, and biodiversity (Hardiman et al., 2011; Homeier et al., 2010; Jung et al., 2012; E. LaRue et al., 2019; Lindenmayer et al., 2000; Lindenmayer, 2019; R. H. MacArthur & MacArthur, 1961; Murphy et al., 2022).

Traditional forest inventory metrics like DBH, tree height, and volume help quantify structural complexity but can be limiting on their own (McElhinny et al., 2005). This is why newer techniques have been developed to capture additional aspects of FSC such as the variation in canopy height and the vertical and horizontal distribution of vegetation (J. Atkins et al., 2018). Remote sensing tools, such as lidar, have proven useful in capturing the three-dimensional structure of forests to estimate FSC that would be either costly or impossible to obtain through traditional forest inventory methods (J. Atkins et al., 2020; Lefsky et al., 1999; Means et al., 2000). For example, lidar can characterize fine vegetation structure and quantify canopy variation that would be difficult to assess through manual measurements (J. Atkins et al., 2018).

As remote sensing and mapping technologies have become more widely available, the number of methods for measuring structural complexity has increased dramatically. Terrestrial and aerial laser scanning (TLS and ALS) have made it possible to obtain accurate three-dimensional data on the structural features of forest stands (E. LaRue et al., 2020; Lefsky et al., 1999). While both tools have drawbacks, they can effectively work in concert with one another (Hilker et al., 2012). Terrestrial laser scanning measures the forest from the ground, and can provide detailed sub-canopy data, but is limited in its ability to measure canopy features due to occluding foliage (Côté et al., 2009; Watt &

Donoghue, 2005). On the other hand, aerial laser scanning measures forest canopy from above, providing highly detailed data on the canopy surface (Hilker et al., 2012). Because of the different perspectives, ALS and TLS can work together to provide a complete picture of forest canopy structure (E. LaRue et al., 2020).

Both aerial and terrestrial laser scanning can provide accurate measurements of canopy height, cover and openness quickly over large areas (Lefsky et al., 1999). It is also possible to measure rugosity, rumple, and other geometric measures of complexity with the aid of laser scanning (Danson et al., 2007; Hardiman et al., 2011; Kane, Bakker, et al., 2010; Kane, McGaughey, et al., 2010). Rumple, which is a ratio of the area of a triangular irregular network (TIN) of treetops to the area of the triangles projected to the forest floor, has commonly been used in measures of structural complexity (Zenner & Hibbs, 2000). Increasing accuracy and availability of these metrics has allowed for more valid measurements of structural complexity.

LiDAR datasets are commonly structured as “point clouds” which are datasets comprised of x, y, and z coordinates of points collected by a lidar instrument. Point clouds offer a three-dimensional visual representation of an area. Using the three-dimensional point data, calculations can be made of a wide range of structural parameters.

Despite the widespread use of lidar and other remote sensing tools to measure the structural complexity of forest ecosystems, there are still uncertainties regarding their scale dependence (J. Atkins et al., 2023). Patterns and processes can vary at different spatial extents (Levin, 1992; Qi & Wu, 1996; Wu, 2004). Two studies focused on the same phenomenon can yield apparently conflicting results because the phenomenon was

observed at two different spatial extents (Wiens, 1989; Wu, 1999). A pattern that exhibits considerable variation at one spatial extent could give the impression of greater uniformity when observed at a different scale (Jackson & Fahrig, 2015).

There is not necessarily a 'correct' scale at which to study forest structural complexity or other ecological phenomena as different spatial extents can reveal different patterns and processes. However, it is important to consider the most appropriate scale for each research question. When assessing the right scale to use ecologists must consider the spatial extent necessary to capture important ecosystem processes, sometimes called the 'scale of effect' (Jackson & Fahrig, 2015), as well as the limitations of their research methods. An important consideration in research methods is the labor cost of the methodology as researchers and technicians are limited by time. In many fields of research, there is usually a necessary trade-off between characterizing a subject at high detail but over a small extent, or low detail over a large extent (J. Atkins et al., 2023). When it comes to assessments of FSC, it appears that there isn't a consistent approach to selecting spatial extent (J. Atkins et al., 2023).

Determining the appropriate scale for an ecological study is critical to the validity of results. Simply choosing the scale at which a relationship displays the highest level of correlation shouldn't be considered adequate (J. Atkins et al., 2023). This approach doesn't necessarily consider all environmental conditions at all extents, nor the extent at which a given environmental variable becomes stable. The concept of representative elementary area (REA), which has been used in hydrology to assess the scale which best represents rainfall-runoff patterns and processes in watersheds. (Wood et al., 1988, 1990). REA, when

applied to other areas of ecology can be defined as the "smallest discernible point which is representative of the continuum" (Wood et al., 1990). This concept can be applied to measures of FSC in order to determine the appropriate scale at which to make measurements.

This study aims to assess the scale-dependency of lidar-derived metrics of structural complexity. Using a range of plot sizes to quantify structural complexity, we hope to gain a better understanding of how certain commonly used metrics and indices respond to scaling.

1.2 Methods

1.2.1 Study Site

This study was confined to the Upper Wild Ammonoosuc (WAMMO) watershed in the White Mountain National Forest (WMNF) (Figure 1). This area was chosen because it contains most forest types found within the WMNF and features topography that is representative of the greater WMNF region. The Upper Wild Ammonoosuc watershed has an elevation ranging from 330 to 1460 meters. Dominant forest types include spruce-fir and maple-beech-birch (McNab et al., 2007).

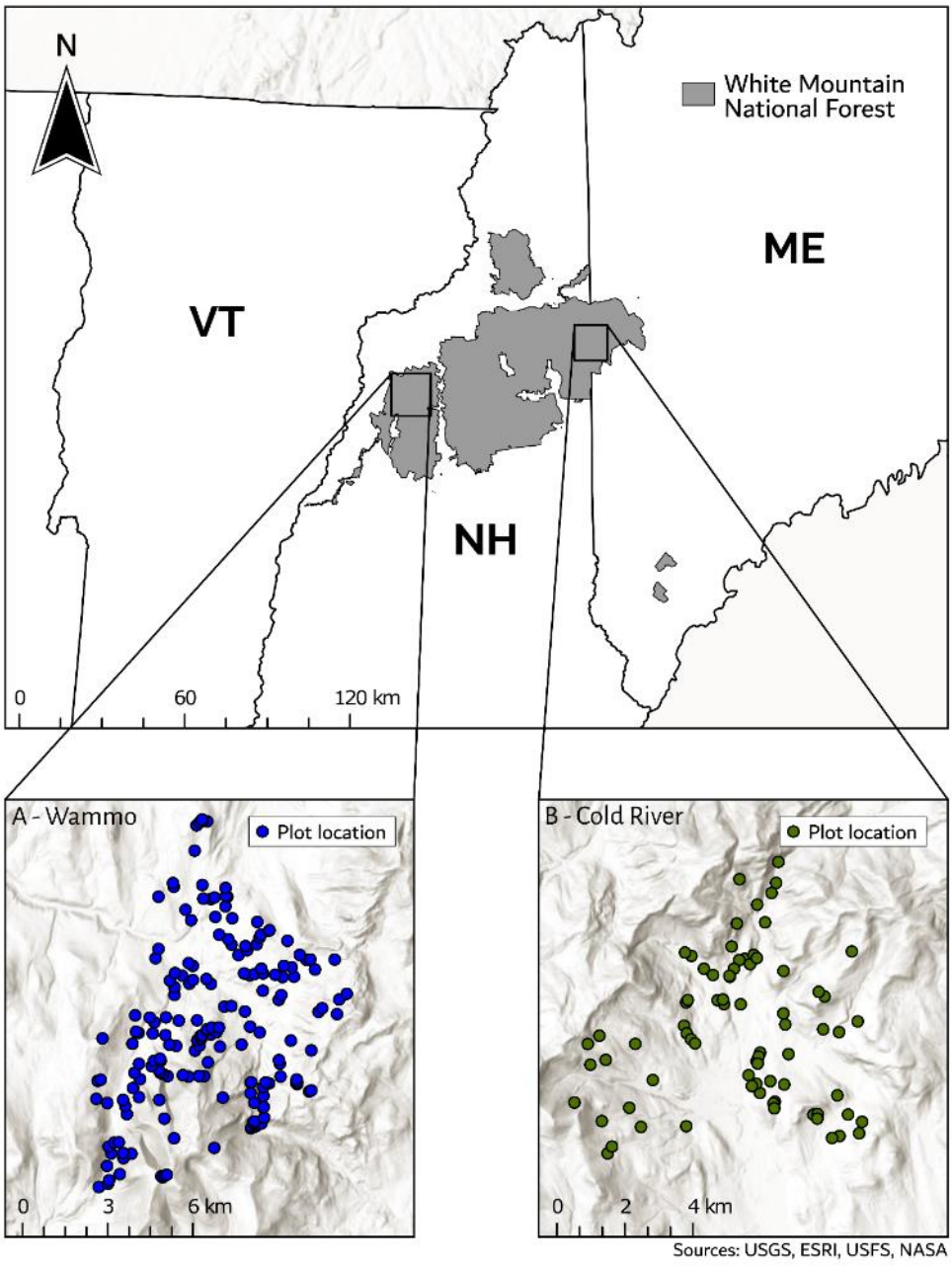

Figure 1 - Map of study area for chapter 1 and chapter 2. A- Upper Wild Ammonoosuc region. B- Cold River region.

1.2.2 Stratified Random Sampling

171 plot centers were selected with a stratified random sampling method to ensure a range of land cover types were represented. Strata were determined by topographic and soil

metrics, which included elevation, slope, aspect, topographic wetness and parent material (Colter, 2019). Strata were first separated into categories based on parent material and then further partitioned into strata based on slope and drainage (Colter, 2019). From this, strata were further divided into categories of timber and non-timber managed areas (Colter, 2019). Ultimately, there were 8 plots per strata, representing a range of vegetation patterns and land cover types. For further explanation, see Colter (2019).

1.2.3 Lidar collection

The lidar data used in this study was collected as part of the Umbagog NH/ME 2016 LiDAR project. The data collection was conducted by Keystone Aerial Surveys, Inc. The prime contractor responsible for all follow-on processing was Quantum Spatial, Inc.

The lidar data acquisition for the whole project took place between spring 2016 and spring 2018, during periods when there was no snow on the ground and rivers were at or below normal levels. The data used for this study comes from the MOD2 site, which was collected during November of 2017. The data covered a partial extent of six counties in New Hampshire and Maine, encompassing approximately 3,276 square miles.

The lidar acquisition specifications varied based on the area of interest. For most areas, a nominal pulse spacing (NPS) of 0.7 meters was used, with a density of 2 pulses per square meter. However, in the White Mountain National Forest NH/ME areas, a finer NPS of 0.57 meters was employed, along with an additional MOD2 WMNF addon area collected at 0.35 NPS. The Riegl Q1560 sensor, with unlimited maximum returns, was used for the MOD2 WMNF addon area.

All lidar data were collected using an airborne platform, with flight parameters set to achieve the desired specifications. The lidar data collection involved the use of three different lidar sensors: the Optech Galaxy T1000, Leica ALS70, and Riegl Q1560. The Optech Galaxy T1000 was operated at a flight height of 2,100 meters, a flight speed of 150 knots, and a scan angle of 20 degrees. It had a scan rate of 53.4 Hz, a pulse repetition rate of 260.4 kHz, a pulse duration of 3 ns, a pulse width of 0.525 microseconds, and a wavelength of 1064 nm. The Leica ALS70 was flown at a flight height of 2,100 meters, a flight speed of 140 knots, and a scan angle of 18 degrees. It had a scan rate of 56 Hz, a pulse repetition rate of 262.6 kHz, a pulse duration of 4 ns, a pulse width of 0.46 microseconds, and a wavelength of 1064 nm. The Riegl Q1560 operated at a flight height of 2,300 meters, a flight speed of 130 knots, and a scan angle of 18 degrees. It had a scan rate of 67.6 Hz, a pulse repetition rate of 251.8 kHz, a pulse duration of 3 ns, a pulse width of 0.58 microseconds, and a wavelength of 1064 nm.

The lidar data used for this study were designated QL1, with a mean point density of 58.5 points/m^2.

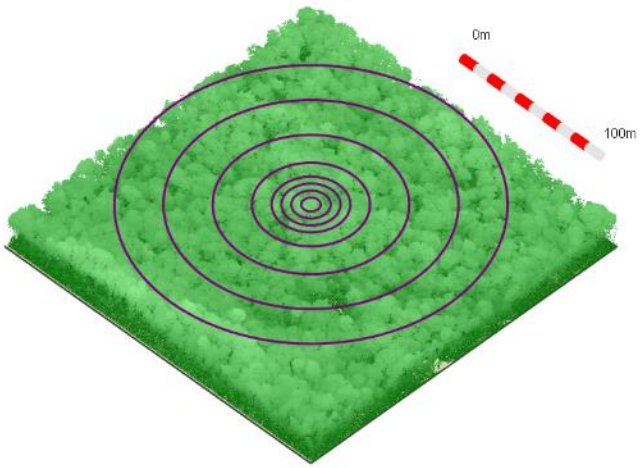

Figure 2 - Depiction of lidar plot sampling methodology. Each plot was measured 8 times around the same plot center coordinates using different radii, ranging from 5 to 100 meters.

1.2.4 Lidar processing and structural complexity metrics

Lidar data were acquired from USGS as LAS files, and processed using the lidR (Roussel et al., 2023) package in R (R Core Team, 2022). Unprocessed LAS files were downloaded as 750m x 750m tiles and subsequently clipped in circles with 125m radii around each plot center, which accounted for a 25m buffer around the largest plot size chosen for this study. To remain consistent with field-measured plots, circular plots were used for lidar-derived metrics of structural complexity. Once clipped, the LAS files were normalized to a TIN-derived digital terrain model, so that a canopy height model relative to an elevation of 0 could be derived.

To assess the relationship between metrics at different extents, each plot consisted of 8 concentric circular boundaries with radii of 5, 10, 15, 20, 30, 50, 75, and 100 meters (see

Figure 2), and each metric was calculated across all plot sizes. 15 lidar-derived metrics were chosen based on their use in previous studies. These metrics included mean outer canopy height, rumple index, rugosity, standard deviation of Z (height of lidar point), entropy, vegetation area index (VAI), vertical complexity index (VCI), foliar height diversity (FHD), 25th and 95th percentile Z, mean crown area, mean gap profile, and a lidar-derived additive structural complexity index. See Table 1 for a full description of each lidar-derived metric.

Table 1 - Description of all lidar-derived metrics of structural complexity

Mean outer canopy height	The mean Z value of first returns that are designated as outer canopy
Maximum canopy height	Maximum Z value
Rumple index	A measure of canopy surface roughness, the ratio of canopy surface area to its projected ground area (Jenness, 2004)
Rugosity	The standard deviation of outer canopy heights (Parker & Russ, 2004).
Z SD	The standard deviation of all Z values in a point cloud.
Entropy	A normalized Shannon vertical diversity index (Li & Reynolds, 1995; Liu et al., 2022; R. MacArthur et al., 1966).
Foliar height diversity	Entropy normalized by maximum canopy height (J. Atkins et al., 2023; R. MacArthur et al., 1966).
Gap fraction profile	An assessment of the number of points that reach a certain layer and those that pass through the layer (Bouvier et al., 2015)
Vegetation area index	The sum of leaf area density, based on the method of Bouvier et al., (2015). It uses gap fraction profile and computes its log divided by an extinction coefficient.
Vertical complexity index	Fixed normalization of entropy from Van Ewijk et al. (2011)
25th percentile Z	25th percentile Z value
95th percentile Z	95th percentile Z value
Maximum crown area	Maximum crown area as calculated by tree segmentation.
Mean crown area	Mean crown area as calculated by tree segmentation.

LASCI	Lidar-derived additive structural complexity index. Uses all lidar-derived metrics and rescales each to a value between 0-10. These are then added together to produce the LASCI value. This is similar to a method described by McElhinny et al. (2006).

1.2.5 Statistical analyses

After calculating all variables for each plot radius, metrics were assessed for pairwise correlations with the corresponding metric at the same plot at all extents used for this study. For this study, we used Pearson correlation coefficient. For example, mean Z calculated for a 5-meter radius plot was compared to the calculation of mean Z at the same plot with all larger radii. This was done to assess the relatedness of each metric to itself at different extents.

Coefficients of variation (CV) were calculated for each metric at each plot size. This was used to assess how variation changed with increasing plot size.

1.3 Results

The WAMMO plots had a mean outer canopy height of 15.35 meters with a 15-meter plot radius, with a range of 3.81 to 22.63 meters across all plots. The foliage height diversity had a range of 1.86 to 3.14, with a 2.77 mean across all plots, while the mean vertical complexity index score was 0.61. See Table 2 for all calculations of the 20-meter radius plot size.

Table 2 - Lidar-derived measurements from 15-meter radius plots

	Mean	Median	Min.	Max.	SD
Mean outer canopy height	15.35	16.19	3.12	22.64	3.82
Maximum canopy height	23.39	24.05	10.49	34.24	4.19
Rumple Index	3.43	3.33	1.97	6.03	0.77
Rugosity	4.02	3.93	1.33	9.37	1.44
Z SD	6.47	6.91	2.16	10.22	1.71
Entropy	0.89	0.89	0.78	0.95	0.04
FHD	2.78	2.82	1.87	3.15	0.20
Gap fraction profile	0.93	0.93	0.87	0.97	0.02
VAI	3.10	3.01	1.06	5.41	0.56
VCI	0.61	0.62	0.41	0.69	0.04
25^{th} percentile Z	4.45	3.99	0.05	13.35	2.37
95^{th} percentile Z	19.02	20.16	6.35	26.47	4.11

Some of the variables had relatively low correlation values when comparing the 5m plot and the 100m plot, like entropy ($r = 0.171$, $p < 0.05$), rugosity ($r = 0.376$, $p < 0.005$), maximum crown area ($r = 0.301$, $p < 0.005$), mean crown area ($r = 0.305$, $p < 0.005$), the standard deviation of crown area ($r = 0.195$, $p < 0.01$). On the other hand, mean canopy height ($r = 0.746$, $p < 0.005$), rumple index ($r = 0.629$, $p < 0.005$), foliar height diversity ($r = 0.665$, $p < 0.005$), 95^{th} percentile Z ($r = .790$, $p < .005$), vegetation area index ($r = 0.682$, $p < 0.005$), and vertical complexity index ($r = .673$, $p < 0.005$) all had higher correlation values between the 5m plot and the 100m plot. In general, correlations between adjacent radii were high, and tended to diverge as the difference in plot size increased. With nearly all variables, the correlation between 5m and 10m plots was the lowest of all adjacent plot radii. For example, the correlation between the rugosity measure at 5m and that at 10m radius was 0.83, while correlations between all other adjacent plot radii were above 0.92. Also, regarding Z percentile, correlations between the smallest and largest plot size increased in value as Z percentile increased.

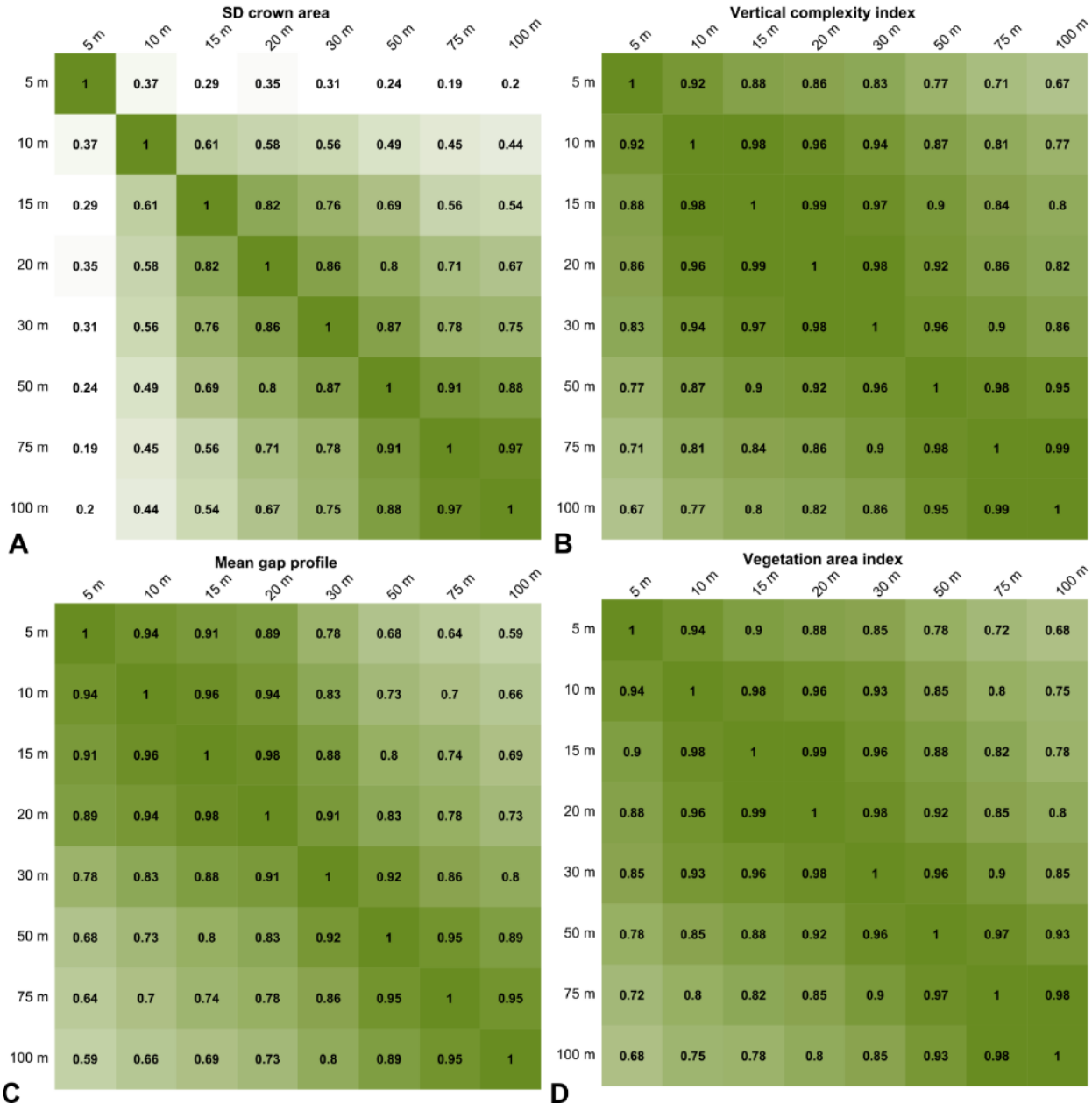

Figure 3 - Correlograms displaying correlations between structural complexity metrics at different plot sizes ($p < 0.01$ for all r-values). A- Standard deviation of crown area. B- Vertical complexity index. C- Mean gap fraction profile. D- Vegetation area index

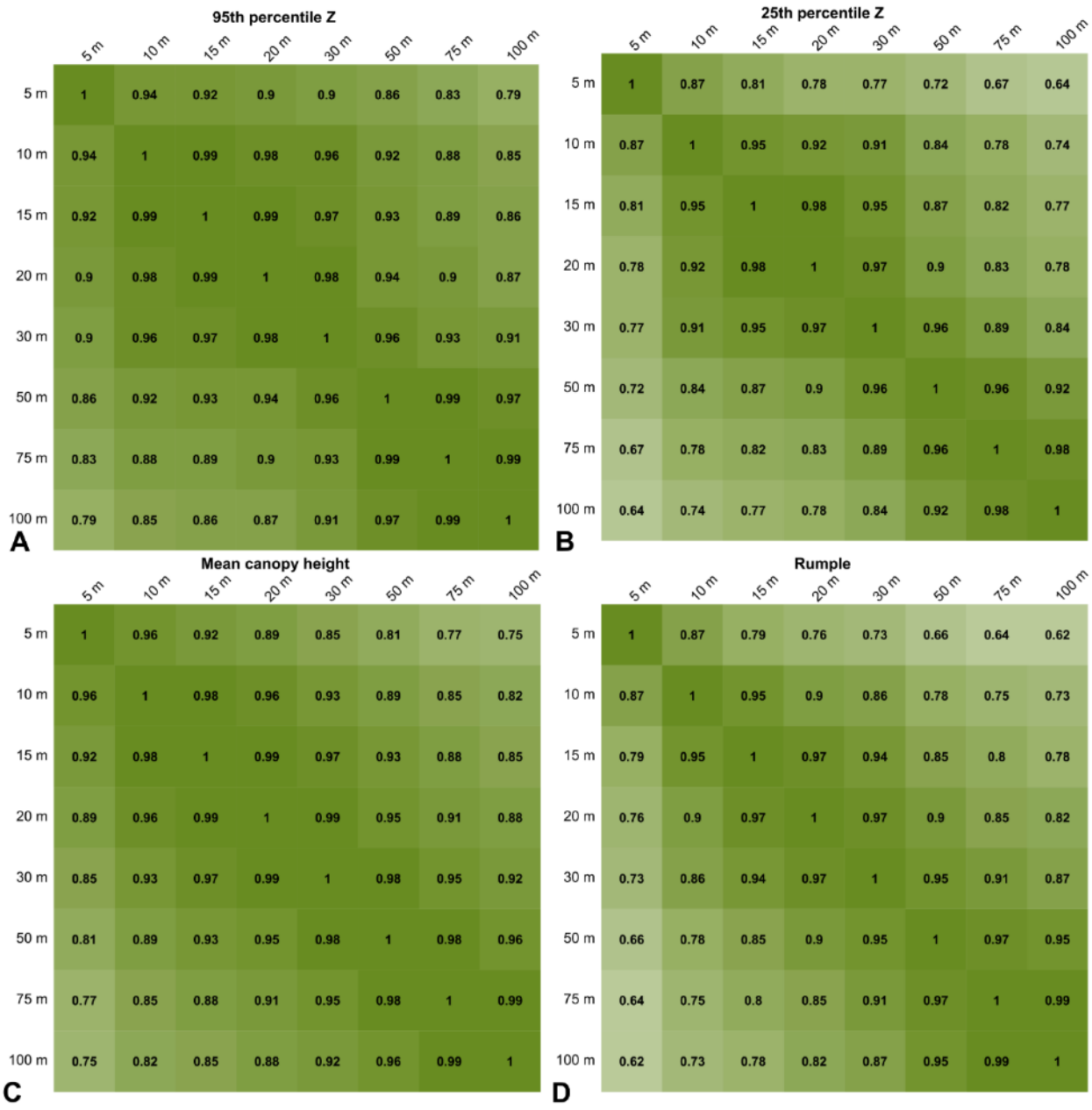

Figure 4 - Correlograms displaying correlations between structural complexity metrics at different plot sizes ($p < 0.01$ for all r-values). A- 95th percentile Z. B- 25th percentile Z. C- Mean outer canopy height. D- Rumple index.

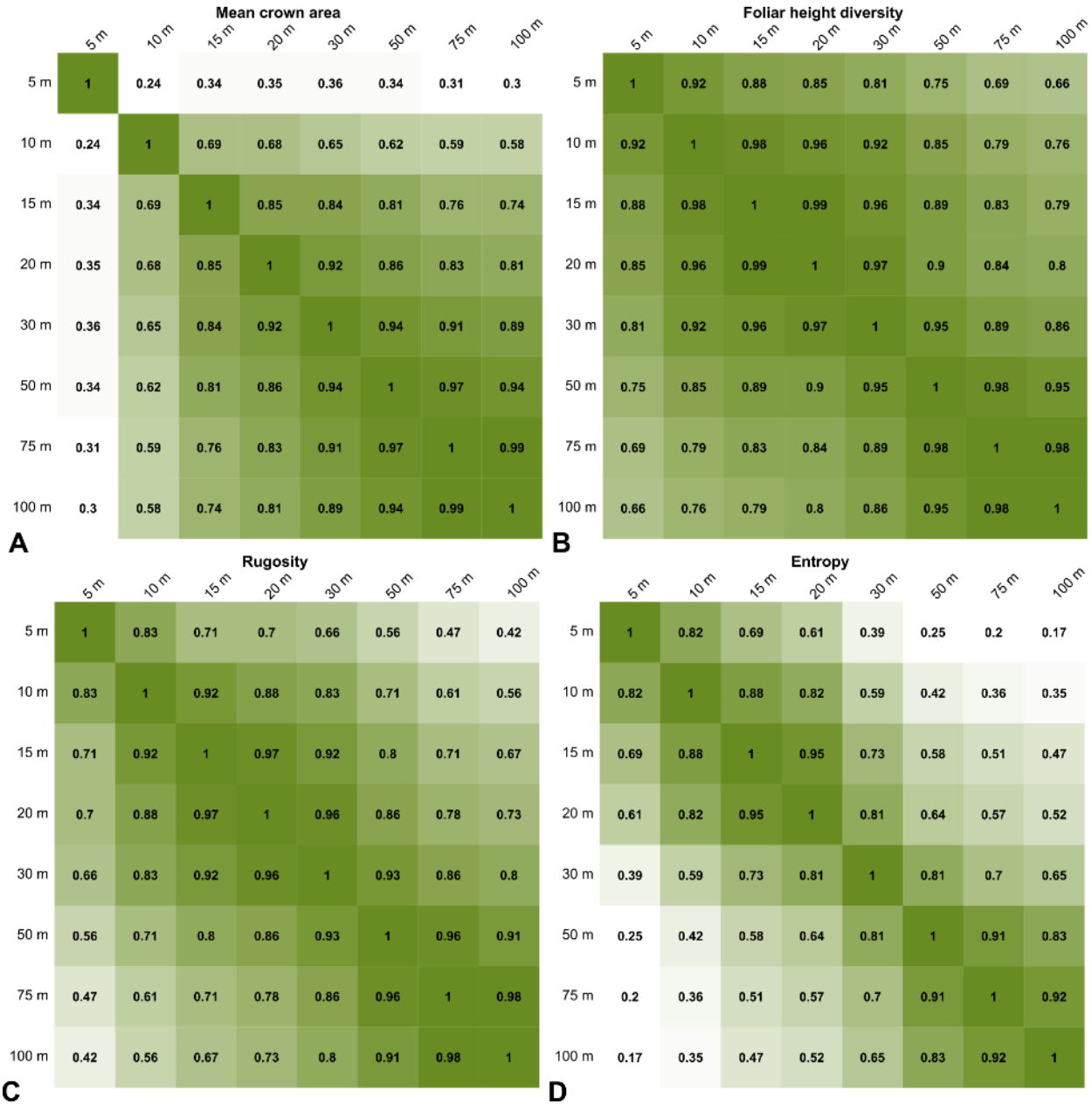

Figure 5 - Correlograms displaying correlations between structural complexity metrics at different plot sizes ($p < 0.01$ for all r-values). A- Mean crown area. B- Foliar height diversity. C- Rugosity. D- Entropy.

Calculations of coefficients of variation (CV) (Table 3, Figure 6) for all variables at each plot size revealed differences in how CV changes as plot size increases. Across nearly all variables used, CV decreased as plot size increased. Furthermore, there were differences among variables in the ratio of the CV at the 100m plot to the CV at the 5m plot. Notably,

the CV for rugosity at 5m was found to be 50.01, while at the 100m plot, it was 30.18. Rumple had a CV of 32.71 at the smallest plot size and 17.50 at the largest. The ratio of CVs at the largest plot size to the smallest plot size was lowest for rumple (0.534), maximum crown area (0.319), mean crown area (0.383), vegetation area index (0.520), the standard deviation of crown area (0.278), and gap profile (0.418). The ratio was highest for mean canopy return height (0.785), 95th percentile Z (0.759), and entropy (0.761). The results here show that there are important differences in the way FSC metrics respond to scaling.

Table 3 - CV% values for each structural complexity metric for each plot size.

Plot radius (m)	5	10	15	20	30	50	75	100
Mean crown area	43.61	24.95	19.81	19.83	18.27	17.98	17.68	16.72
Mean outer canopy height	28.63	25.64	24.97	24.94	25.33	25.21	24.34	23.30
Maximum canopy height	20.88	18.99	18.25	18.03	17.15	16.21	15.04	13.93
Rumple index	32.57	25.08	23.42	22.40	20.69	18.56	17.59	16.86
Rugosity	49.66	41.93	37.81	36.09	33.91	32.40	30.63	29.24
SD Z	28.77	27.25	26.72	26.45	25.91	24.83	23.61	22.65
Entropy	5.98	4.67	4.53	4.25	4.40	4.52	4.34	4.09
Foliar height diversity	8.65	7.71	7.38	7.29	7.12	6.89	6.30	5.77
Gap profile	3.32	2.62	2.30	2.09	1.86	1.61	1.49	1.32
Vegetation area index	24.11	20.18	19.21	18.20	16.54	14.97	13.58	12.54
Vertical complexity index	8.23	7.38	7.17	7.01	6.66	6.23	5.65	5.23
Maximum crown area	32.82	23.35	18.86	17.37	15.45	12.60	10.72	9.46
SD crown area	59.18	34.82	25.71	23.07	19.76	17.63	16.35	15.80
25th percentile Z	67.18	56.91	54.45	53.29	51.23	46.82	43.57	41.43
95th percentile Z	23.58	22.30	21.86	21.73	21.33	20.56	19.52	18.57

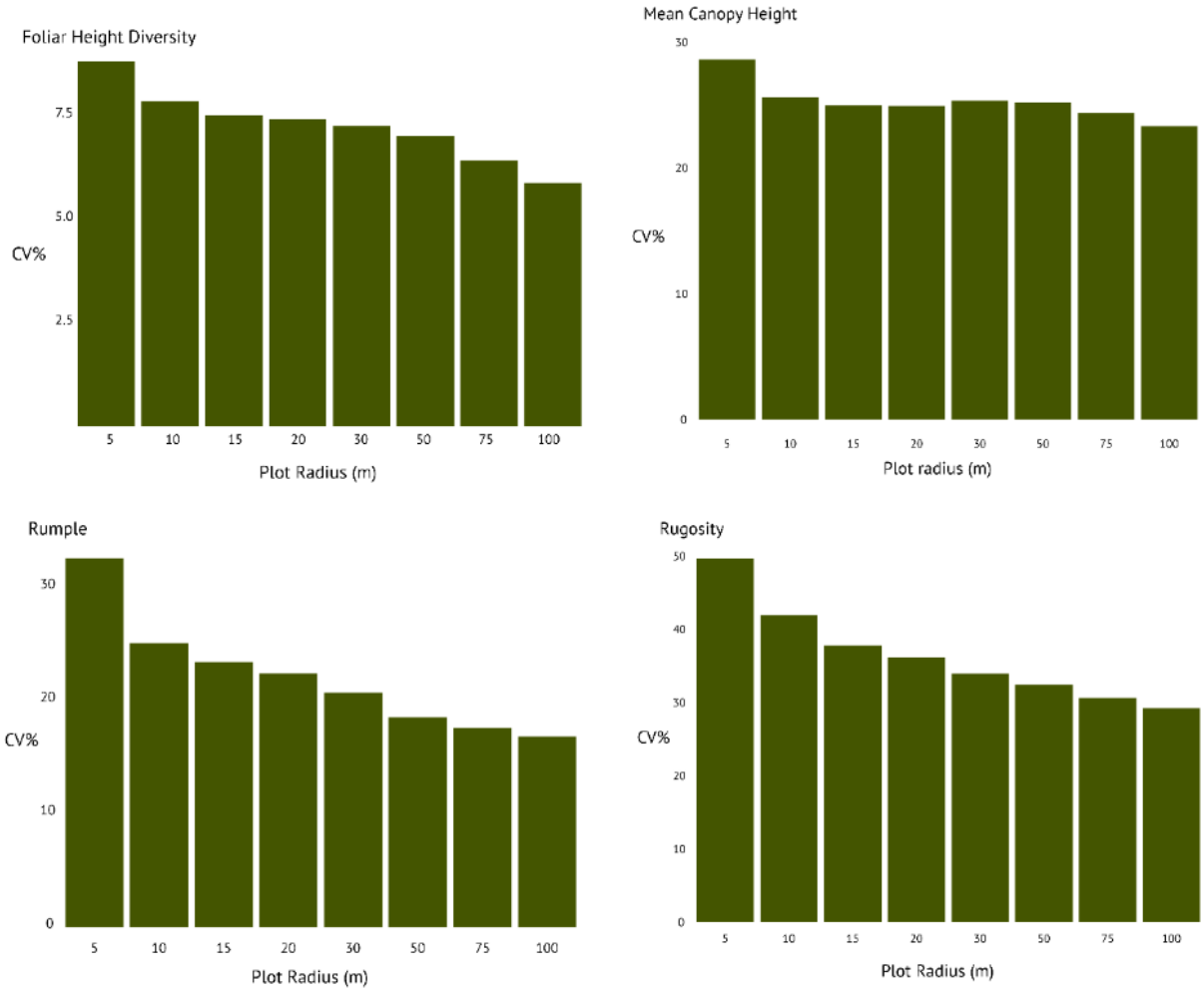

Figure 6 - Graphs of coefficients of variation for selected metrics at each plot size. For all calculated CVs, see Table 3.

1.4 Discussion

As ecological data are becoming more easily accessible, it is important to consider the quality and utility of available data (Nagy et al., 2021). Given that the data used in this study were used in large part because they were freely available for download, some of the motivation behind this study was to expand upon existing standards and to inform future studies. An initial exploration into these data prompted the driving question for this study:

is there an appropriate extent at which to measure aspects of structural complexity in forest sampling using lidar?

There are many studies that have explored the use of lidar in characterizing forest structure (e.g., Atkins et al., 2018; Lefsky et al., 1999; Lim et al., 2003; Nelson et al., 1984). While several studies have sought to refine the criteria for acceptable lidar standards for use in forest inventories (e.g., Gobakken et al., 2008; Hayashi et al., 2014; E. A. LaRue et al., 2022), the question of spatial extent remains cloudy. While there have been studies that explored the relationship between other forest characteristics and lidar data spatial extent , there have been relatively few studies that sought to understand the effect of scaling on FSC metrics (J. Atkins et al., 2023; Bankston et al., 2021; Chungan Li et al., 2022; Deo et al., 2016; Frazer et al., 2011).

All metrics used in this study have been previously used in lidar-based assessments of structural complexity. The high correlation values between the smallest and largest plot sizes for some of these metrics are somewhat surprising given the dramatic difference in area covered by these plots. For reference, a plot with a 100-meter radius has 400x the area of a plot with a 5-meter radius. With correlation values approaching .8 for some of these metrics, it stands to reason that smaller plot sizes can be sufficient for representing larger areas, depending on which metrics one is using. Given the computational demand of processing lidar data, especially high-density lidar, this result is important, and it may lead to less time spent processing lidar data. One of the major reasons for the proliferation of the use of lidar data in forest ecology is the relatively low labor cost involved in collecting

data (Hummel et al., 2011). However, the cost is not insignificant when it comes to both the financial and labor investment in collecting and processing lidar data (Jeong et al., 2018).

In this study, the high correlation values between the smallest and largest plot sizes for some of these metrics are somewhat surprising given the dramatic difference in area covered by these plots. A plot with a 100-meter radius has 400x the area of a plot with a 5-meter radius. With correlation values approaching .8 for some of these metrics, it stands to reason that smaller plot sizes can be sufficient for representing larger areas, depending on which metrics one is using. Given the computational demand of processing lidar data, especially high-density lidar, this result is important, and it may lead to less time spent processing lidar data.

It is worth noting that the differences in how these metrics scale is not indicative of any one metric being "better" than any other. For example, the lower correlation between rugosity of the 5m plot and rugosity of the 100m plot compared to the correlation between rumple indices at the smallest and largest plots doesn't necessarily mean that rumple is more useful a metric than rugosity. However, it does shed some light on the appropriate uses of each metric. In this example, one takeaway could be that rugosity might be a better metric to use for fine-scale assessments of FSC, while rumple index might be a more useful metric for extrapolating information from small plots to the larger stand. Ultimately, this indicates that the REA differs between metrics. Wood et al. (1988), in their study and introduction of the concept of REA in the context of hydrology posit that REA can vary and is influenced by a variety of factors, like topography. When it comes to determining REA for forests, this is

likely to be the case as well, and this study helps elucidate which factors to consider when determining REA in this region.

These results can help determine the REA for FSC metrics of interest in New England mixed hardwood forests. While this study will shed light on how spatial extent affects FSC metrics generally, researchers should proceed with caution as this study only focused on one region in the WMNF. Forest structure varies significantly across forest types, and it has already been found that REA will vary in different forest types, too (J. Atkins et al., 2023).

This study did not explore the relationships between the FSC metrics and other ecological variables (e.g., wildlife interactions) at different spatial extents, but this would be a worthwhile future direction. Determining the scale of effect that some of these metrics have with other variables will also be useful in establishing methodologies for using lidar in ecological studies (Jackson & Fahrig, 2015).

1.5 Conclusions

For many of these metrics with high correlation values between the smallest and largest plots, the 5-meter radius plot might be a sufficient REA. However, other aspects of FSC will require larger extents for their REA. This is a promising finding for the practical implementation of FSC metrics in forest management and conservation. This should lead to less time and lower cost of processing lidar data for FSC metrics.

2 CHAPTER 2: Forest structural complexity metric relationships and the compatibility of field and lidar-derived variables in New England mixed hardwood forests

2.1 Introduction

Understanding forest structure is critical to sustainable forest management. The growing knowledge of forest structural complexity has led to an increasing emphasis on creating complex forest stands to promote ecosystem resilience, ecosystem function, productivity, carbon storage, and biodiversity (Hardiman et al., 2011; Homeier et al., 2010; Jung et al., 2012; E. LaRue et al., 2019; Lindenmayer et al., 2000; Lindenmayer, 2019; R. H. MacArthur & MacArthur, 1961; Murphy et al., 2022). As a result, there is now an understanding that complexity is an informative characterization in forest management (Fahey et al., 2018; Puettmann & Messier, 2019).

A common goal of sustainable forest management is the conservation of biodiversity. In looking at forest structure, it is possible to identify attributes of a forest that broadly impact biodiversity (Lindenmayer et al., 2000). It has been shown that species richness is correlated with spatial heterogeneity in ecosystems (Stein et al., 2014), although there can be variation between species groups (Tews et al., 2004). There are also many known links between certain forest structural attributes and the presence and abundance of certain species (Gibbons et al., 2002; Jung et al., 2012; R. H. MacArthur & MacArthur, 1961). Early work by MacArthur et al. (1966) showed a connection between vertical forest structure (i.e., the arrangement of branches in a forest) and bird abundance. It has been found more recently that a more structurally complex forest can lead to increased diversity of bats (Jung et al., 2012).

Beyond biodiversity, forest structural complexity can have a broad impact on the resilience and function of a forest ecosystem (Fahey et al., 2015). Generally, though with some exceptions, ecosystems with more plant diversity exhibit higher net primary production (Hooper et al., 2005). The relationship between structure, function, and productivity has only more recently been extensively researched. It has been shown that there is a correlation between certain structural complexity metrics and rates of primary production (Gough et al., 2016, 2019; Hardiman et al., 2011) and ecosystem function (E. LaRue et al., 2019). One study found that in some forest systems, canopy rugosity is positively correlated with net primary production (Gough et al., 2019). Resource-use efficiency, specifically light and water, has also been shown to be correlated with structural complexity (J. W. Atkins et al., 2018; Murphy et al., 2022)

As climate change progresses, another common goal of sustainable forest management is maximizing carbon sequestration and storage in an effort to mitigate the effects (Bravo et al., 2008; Johnson & Curtis, 2001; Lal, 2005; Nunery & Keeton, 2010). Forests have the potential to sequester and store large amounts of carbon, and efforts to maximize carbon storage could have global effects. It has been shown that more structurally complex, late-successional and old growth forests tend to have higher above-ground carbon stocks than early- or mid-successional forests (Gunn et al., 2014; Thom & Keeton, 2019). Although, this isn't always the case. For example, in the northeast United States, stands affected by spruce budworm can exhibit higher rates of mortality decades after defoliation (Taylor & MacLean, 2009). To better understand the effects of structural complexity on carbon storage dynamics, the relationship between complexity and stand age must also be better understood. Currently, it is unclear to what extent structural complexity increases with

stand age. It has been suggested that, in some cases, forests with old-growth attributes aren't necessarily more complex than stands in earlier successional stages (Zenner, 2004), even though some studies suggest that structural complexity can increase with stand age (Bradford & Kastendick, 2010). So, it is important to better understand the relationship between structural complexity and development stage.

Quantifying structural complexity in a forest can be challenging due in part to the number of attributes used, along with a lack of clarity around what exactly is meant by "complexity" (Loke & Chisholm, 2022). In addition, it is not easy to define complexity, and, in ecology, has often been used interchangeably with diversity and heterogeneity, which adds to the ambiguity (Li & Reynolds, 1995; Loke & Chisholm, 2022).

Many approaches can be used to measure structural complexity (McElhinny et al., 2005; Pommerening, 2002; Staudhammer & LeMay, 2001). Early measurements of complexity involved direct measurements of structural components such as foliage height diversity (R. H. MacArthur & Horn, 1969). However, as the literature on FSC has expanded, and newer technology became available, the number of attributes comprising a FSC assessment has grown. The list of attributes historically used to measure FSC is too long to list here. Still, much of the available literature has included metrics of canopy strata (e.g., MacArthur & MacArthur, 1961), tree dbh (e.g., Franklin & Spies, 1991), tree heights (e.g., DeWalt et al., 2003), basal area of large trees (e.g., Franklin & Spies, 1991), and deadwood components (e.g., Gibbons et al., 2002).

Some measures of FSC use diversity indices to assess the diversity of measurable stand attributes like dbh, total heights, or foliage heights (Schulte & Buongiorno, 1998;

Staudhammer & LeMay, 2001). The Shannon index, commonly used to quantify species diversity, has also been used to assess structural attributes' diversity (Buongiorno, 2001; Schulte & Buongiorno, 1998). This requires breaking down continuous variables, like dbh and height, into discrete bins or classes, which involves some degree of subjectivity in deciding the intervals to use. Rather than using the proportion of individuals in each diameter or height class, when assessing structural diversity, the index is based on the proportion of basal area within each bin.

Not all indices are equal, of course, and it has been argued that some are more effective than others when assessing structural complexity (Lexerød & Eid, 2006; Loke & Chisholm, 2022). It has been suggested that diversity indices may be insufficient for measuring structural complexity, and that measures of equitability, such as the Gini coefficient, are more useful to employ (Valbuena et al., 2012). The Gini coefficient has historically been used to describe wealth and income inequality (e.g., Dasgupta et al., 1973). However, more recently, it has also been applied to measure structure in plant communities (Weiner & Solbrig, 1984). One of the arguments for using the Gini coefficient over other diversity indices is that it has been found to discriminate more effectively between varying diameter distributions (Lexerød & Eid, 2006). It can also be argued that the ranking of equitability produced by measuring the Gini coefficients of diameter distributions in different forest stands is logical and easy to interpret, with a value of 1 indicating a highly even distribution across size classes, and 0 indicating nearly all trees falling into one size class (Lexerød & Eid, 2006).

Given the seemingly endless methods of quantifying FSC, it is a worthwhile endeavor to assess commonly used metrics. Many of these metrics may be used interchangeably to an extent, despite the findings that suggest different metrics reveal different aspects of forest structure (Valbuena et al., 2012). It is important to understand these applications of measurements of FSC to better serve the needs of forest management. The relationships between metrics of FSC are also not well understood. Specifically, the relationship between traditional field-based metrics of FSC, and lidar-derived metrics of FSC is an area that should continue to be explored.

This study evaluates some commonly used metrics of FSC, assessing the relationship between field-based and lidar-derived metrics. It also evaluates the validity of metrics of FSC to help determine the appropriateness of these metrics in the context of forest structural assessments. Here, we intend to identify and analyze various metrics and determine their strengths and limitations in capturing FSC. Furthermore, we investigate the degree of complementarity between field- and lidar-derived metrics of FSC. Overall, this study aims to analyze and compare different metrics and approaches to measuring FSC to determine their suitability for characterizing forest structure.

2.2 Methods

2.2.1 Study site and stratified random sampling

This study took place within two primary locations in the WMNF, the Upper Wild Ammonoosuc watershed (WAMMO) and the Cold River (CR) region. Both WAMMO and CR

were chosen because they exhibit a range of forest types and topography that are representative of the WMNF. The WAMMO watershed and CR region have an elevation ranging from 330 to 1460 meters. Dominant forest types include spruce-fir and maple-beech-birch (McNab et al., 2007). For additional details on the WAMMO site, refer to chapter 1.

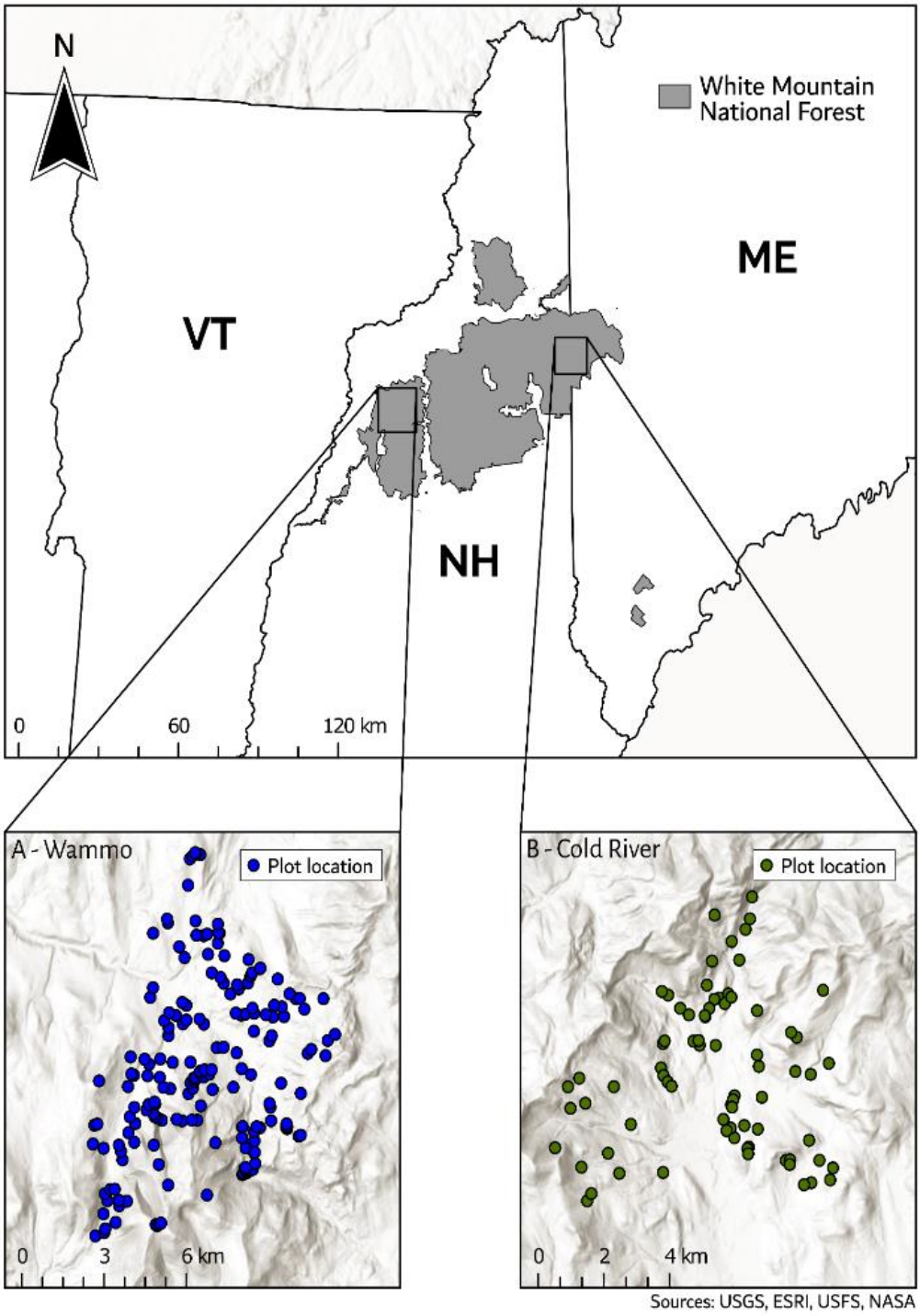

Figure 7 - Map of study area for chapter 1 and chapter 2. A- Upper Wild Ammonoosuc region. B- Cold River region. In the WAMMO region, both QL1 and QL2 lidar data were used. In the Cold River region, only QL2 lidar data were used.

At the WAMMO site, 171 plot centers were selected with a stratified random sampling method. Strata were determined by topographic and soil metrics. For additional details on sampling stratification, see Colter (2019).

At the CR site, 75 plot centers were selected with a similar stratified random sampling method, which was determined by topographic and soil metrics.

2.2.2 Lidar collection

The QL1 lidar data used in this study for the WAMMO region and the QL2 lidar data for the CR region were collected as part of the Umbagog NH/ME 2016 LiDAR project. The data collection was conducted by Keystone Aerial Surveys, Inc. The prime contractor responsible for all follow-on processing was Quantum Spatial, Inc.

The lidar data acquisition took place between spring 2016 and spring 2018, during periods when there was no snow on the ground and rivers were at or below normal levels. The data covered a partial extent of six counties in New Hampshire and Maine, encompassing approximately 3,276 square miles. For specifications of instruments used, refer to chapter 1.

Most of the lidar data acquired for this study was designated QL2, but a section of the WMNF, section MOD2, was designated QL1. The lidar data that were designated QL1, with a mean point density of 58.5 points/m^2. The QL2 lidar data had a mean point density of 7.22 points/m^2. In the WAMMO region, both QL1 and QL2 lidar data were used.

The QL2 lidar data used in this study for the WAMMO region were obtained from Photo Science, Inc. as part of the White Mountain National Forest Lidar project. The project aimed

to collect lidar data for a high-resolution dataset covering an Area of Interest (AOI) of approximately 187 square miles within the White Mountain National Forest in New Hampshire. The lidar data collection was carried out between November 2010 and April 2012, during periods when there was no snow on the ground and rivers were at or below normal levels.

The lidar data were collected using an airborne platform and followed the U.S. Geological Survey National Geospatial Program Base LIDAR Specification, Version 13. The data acquisition involved a nominal pulse spacing (NPS) of 1.0 meter to ensure high-resolution coverage of the study area. The data were collected in raw flightline swath format using an Optech sensor.

The lidar data were developed based on a horizontal projection and datum of UTM NAD83, UTM Zone 19, in meters. The vertical datum used was NAVD1988 (GEOID09) in meters. The lidar data were processed to create classified LAS 1.2 files, which were formatted into individual 2000m x 2000m tiles. Corresponding 1.0 meter gridded Raster DEM Files were also created and tiled to the same 2000m x 2000m standards.

The lidar data processing and analysis were conducted using various software tools, including MicroStation Version 8, TerraScan Version 12, TerraModeler Version 12, GeoCue Version 2011.1.20.3, ESRI ArcGIS 10.0, and Global Mapper 13. Optech DashMAP 5.2000 software was used for the initial calibration of the lidar data.

The raw flightline LAS files were used to create various project-specific datasets, including intensity images, tiled LAS files, breaklines, bare-earth DEMs, triangular irregular networks (TINs), and fully classified LiDAR LAS files. The classified LAS files represented the

manually reviewed bare earth surface, which facilitated the creation of intensity images, breaklines, and raster DEMs. The raster DEM files, in turn, were used to visualize the digital elevation model of the LAS Class 2 surface and generate contours.

2.2.3 Lidar processing and structural complexity metrics

Lidar data were acquired from USGS as LAS files, and processed using the lidR (Roussel et al., 2023) package in R (R Core Team, 2022). Unprocessed LAS files were downloaded as 750m x 750m tiles and subsequently clipped in circles with 125m radii around each plot center, which accounted for a 25m buffer around the largest plot size chosen for this study. To remain consistent with field-measured plots, circular plots were used for lidar-derived metrics of structural complexity. Once clipped, the LAS files were normalized to a TIN-derived digital terrain model, so that a canopy height model relative to an elevation of 0 could be derived.

Structural complexity metrics were calculated using the lidR package (Roussel et al., 2023). The specific metrics calculated were chosen because of their use in previous studies. The metrics included mean Z, rumple index, rugosity, standard deviation of Z, entropy, vegetation area index (VAI), vertical complexity index (VCI), foliar height diversity (FHD), 25^{th} and 95^{th} percentile Z, mean crown area, mean gap profile, and a lidar-derived additive structural complexity index. For more detail on lidar-derived metrics, see chapter 1 and Table 2.

2.2.4 Field Sampling

At each plot, field crews performed a nested plot inventory. Within a 4.23-meter radius, all living and dead woody stems between 2.5 cm and 12.6 cm DBH were tallied and their DBH was measured. Within a 10-meter fixed radius plot, all stems 12.7 cm to 30.0 cm DBH were tallied. For stems 30.1 cm DBH and larger, a Spiegel-relascope with a metric BAF 2.25 m^2/ha was used to tally trees. For all trees counted as "in" with a metric BAF 4 m^2/ha, total height, height to base of crown, and crown radius were measured.

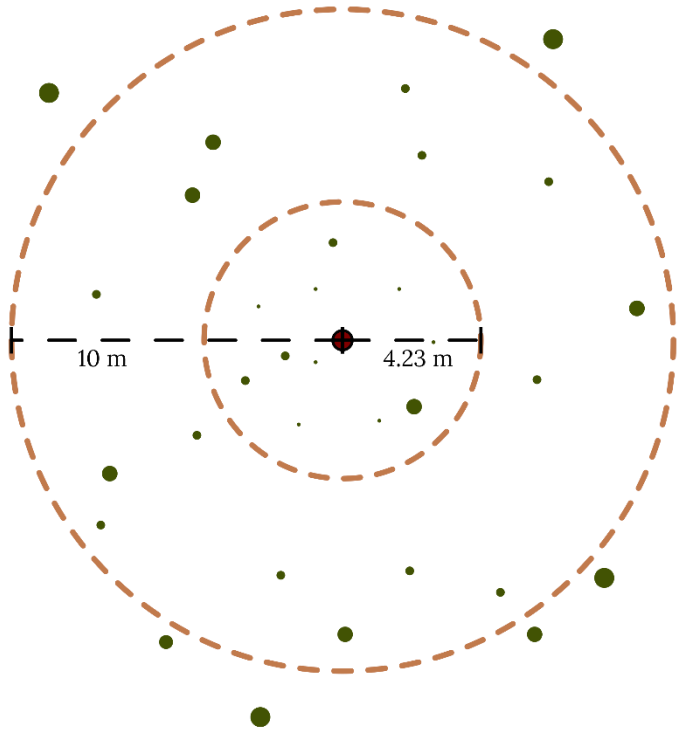

Figure 8 - Diagram of field sampling methodology. Two nested, fixed radius plots with additional prism sampling (BAF 2.25) beyond outer plot radius.

2.2.5 Field-derived measurements and calculations

From the measurements made in the field, we made additional calculations on stand characteristics. These included trees per hectare, standing dead (snags) trees per hectare, basal area per hectare (m^2/ha), snag basal area per hectare (m^2/ha), additive stand density index (ASDI), and the ratio of ASDI to stand density index (SDI) (1-ASDI/SDI).

Table 4 - Description of field-derived metrics used in this study.

Trees/ha	Estimated number of individual trees per hectare at each plot.
Snags/ha	Estimated number of standing dead trees per hectare at each plot.
BA/ha	Estimated total combined basal area, or cross-sectional area at breast height, at each plot.
Snag BA/ha	Estimated total combined basal area of standing dead trees at each plot.
QMD	Quadratic mean stem diameter at breast height.
ASDI	Additive stand density index, calculated as $$\sum N_i(\frac{D_i}{D_r})^a$$ Where i indicates the stand's ith component, N_i is the number of trees per hectare, D_i is the diameter of the ith component, and D_r is the reference diameter, which is 25 cm if using metric units. a is a constant, for which 1.605 was used. (Curtis, 1970; Long & Daniel, 1990)
1 - (ASDI/SDI)	The ratio of ASDI to traditional stand density index (Ducey, 2009; Reineke, 1933)
Trees/ha >40cm	Estimated number of individuals with DBH greater than 40 cm.
DBH class H'	Diameter class diversity index. Uses Shannon's index to calculate probability that a random individual picked would come from a certain diameter class. Diameter classes were made up of 10 cm ranges (e.g., 0-10, 10-20, 20-30 cm, etc.) Proportion of the total population was calculated using basal area.
Species H'	Shannon's diversity index of species.
DBH class Gini coefficient	A measure of inequality or evenness across diameter classes (Dasgupta et al., 1973; Loke & Chisholm, 2022). Calculated using DescTools (Signorell, 2022)

FASCI	Field-derived additive structural complexity index (see LASCI for calculation).
ASCI	Additive structural complexity index; the sum of FASCI and LASCI.

Additionally, several metrics were calculated to characterize the complexity of the plot, which included Shannon's index of DBH class (DBH class H'), species H', Gini coefficient of DBH class, and a field-derived additive structural complexity index (FASCI). FASCI was calculated by rescaling all listed metrics to fall between 0 and 10, and then adding them together. The inclusion of this novel additive structural complexity index is not necessarily to suggest that it be used by others to assess FSC. Rather, it is intended to illuminate the relationships between lidar-derived metrics and field-derived metrics of FSC.

To calculate DBH class H', trees were separated into DBH classes made up of 10cm intervals. We calculated DBH class H' using the proportion of basal area in each DBH class. The number of large diameter trees was also calculated, as they can be an important indicator of forest structure (Lutz et al., 2018). For this study, 40 cm was chosen as the threshold for "large-diameter" trees. According to a study by Lutz et al. (2018), the threshold for "large-diameter" trees in this region was 37 cm, but we rounded up because we were using dbh class bins of 10 cm intervals. Gini coefficient of DBH class was calculated using the DescTools R package (Signorell, 2022). For full description of metrics calculated, see Table 4.

2.2.6 Data analysis

Summary statistics for each metric were calculated. Then the calculated metrics were analyzed using a series of principal components analyses. A PCA of the QL1 metrics alone,

QL2 metrics alone, QL1 metrics with field-derived metrics, and QL2 with field-derived metrics was used to assess the relationships between the FSC variables. PCAs were computed using the FactoMineR R package (Le et al., 2008), and visualizations were created using the factoextra R package (Kassambara & Mundt, 2020). For the PCAs which analyzed lidar- and field-derived metrics together, 11 metrics from each category, plus the associated additive indices were used. The variable contributions and correlation values with primary axes were also calculated.

2.3 Results

2.3.1 Field and lidar calculations

At the WAMMO site, the mean trees above 2.5 cm dbh per hectare found across all plots was 2660.15, while the total basal area had a mean value of 35.73 m^2/ha. The quadratic mean diameter across all plots was found to be 15.47 cm. The mean number of large-diameter trees was 15.94 per hectare. The Shannon's index of DBH class had a mean value of 1.46 with a range from 0.62-2.01. From the QL1 lidar data, a mean outer canopy height of 15.43 was found across all plots. A range of vertical complexity index values between 0.42 and 0.69 with a mean of 0.61. The mean rugosity was 3.84, while the mean rumple index was 3.41. For detailed summary statistics, see Table 5.

Table 5 - Field- and QL1 lidar-derived metrics from WAMMO site.For full explanations of metrics, see Table 1 and Table 4.

	Min.	Max.	Median	Mean	SD
Lidar-derived metrics					
Mean outer canopy height (m)	3.16	22.60	16.41	15.43	3.83
Max. canopy height (m)	10.41	31.07	23.63	22.78	4.12
Rumple	1.90	5.98	3.23	3.41	0.80
Rugosity	1.24	8.97	3.71	3.84	1.44

Entropy	0.75	0.96	0.89	0.89	0.04
SD Z	2.17	10.05	6.84	6.44	1.71
VAI	1.05	5.75	3.01	3.13	0.60
VCI	0.42	0.69	0.61	0.61	0.04
SD crown area	5.30	28.17	16.37	16.13	4.11
Foliar Height Diversity	1.87	3.17	2.80	2.76	0.20
25th Percentile Z (m)	0.06	14.04	4.07	4.53	2.47
95th Percentile Z (m)	6.42	26.25	20.08	18.91	4.11
Mean crown area	14.00	51.35	33.93	33.96	6.74
Mean gap profile	0.87	0.97	0.93	0.93	0.02
LASCI	56.05	111.78	97.17	94.24	9.72
Field-derived metrics					
Trees/ha	228.02	18267.2	2001.04	2660.15	2601.15
Snags/ha	0	3711.19	185.12	353.99	509.95
BA/ha (m^2/ha)	0.97	83.89	34.28	35.73	13.06
Snag BA/ha (m^2/ha)	0	22.21	4.13	5.14	4.55
QMD (cm)	5.65	37.06	13.92	15.47	5.63
ASDI	133.48	8859.55	2113.94	2449.75	1376.55
1 - (ASDI/SDI)	0.04	0.57	0.32	0.31	0.12
Trees/ha >40cm DBH	0	45.29	14.63	15.94	12.12
DBH class H’	0.62	2.01	1.5	1.46	0.28
species H’	0	2.04	1.13	1.12	0.39
DBH class Gini coefficient	0.19	0.61	0.31	0.32	0.06
FASCI	30.82	79.62	66.83	65.85	7.63
ASCI	74.49	168.01	146.45	143.96	13.18
Point cloud density (points/m^2)	30.45	86.02	57.64	58.59	11.75

The QL2 lidar data for the WAMMO region showed a mean outer canopy height of 12.56. The mean rumple index was 4.77, while the mean rugosity was 5.35. Across these plots with this set of lidar data, VCI was measured to have a mean of 0.55. The point cloud density for this region had a mean value of 5.63 points/m^2.

Table 6 - QL2 lidar-derived calculations for WAMMO region. For field-derived metrics, see Table 5.

	Min.	Max.	Median	Mean	SD
Lidar-derived metrics					
Mean outer canopy height (m)	0.52	21.12	12.59	12.56	3.64
Max. canopy height (m)	5.56	35.1	22.39	21.62	3.64
Rumple	1.34	10.99	5.08	5.35	1.98
Rugosity	0.87	9.54	4.64	4.77	1.81

Z SD	0.47	0.94	0.85	0.82	0.09
Entropy	1.12	10.25	6.70	6.52	1.74
VAI	0.13	4.38	2.37	2.44	0.73
VCI	0.18	0.67	0.56	0.55	0.07
Mean crown area (m^2)	0.73	49.40	25.43	25.07	8.50
SD crown area	2.77	21.14	11.62	11.58	3.66
Foliar Height Diversity	0.80	3.06	2.53	2.51	0.32
25th Percentile Z (m)	0.02	9.97	0.43	1.90	2.17
95th Percentile Z (m)	3.25	25.10	19.08	18.16	4.10
LASCI	15.78	86.69	68.67	67.87	9.34
Point cloud density (points/m^2)	0.92	13.36	5.15	5.63	1.97

The CR region had a mean value of 1738.85 trees with a DBH above 2.5 cm, per hectare, a mean total basal area of 35.20 m^2/ha. The quadratic mean diameter across all plots was 18.64 cm. The mean Shannon's index of DBH class value was 1.51 with a range of 0.54 to 2.08. With large-diameter trees, a mean value of 21.69 individuals per hectare was found.

The QL2 lidar data from the CR region had a mean value of 7.22 points/m^2. Regarding lidar-derived metrics, a mean outer canopy height of 11.34 meters was found across all plots. The mean 95th percentile Z value was 18.97 meters. The mean crown area of crowns measured was 22.94 m^2. The VCI calculated in the CR region ranged from 0.15 to 0.68, with a mean value of 0.53. For additional details, see Table 7.

Table 7 - Field- and QL2 lidar-derived calculations from the Cold River region.

	Min.	Max.	Median	Mean	SD
Lidar-derived metrics					
Mean outer canopy height (m)	0.64	21.43	11.24	11.34	3.69
Rumple	1.93	12.10	7.64	7.23	2.43
Max. canopy height	9.36	38.02	23.11	23.1	4.62
Rugosity	1.96	12.84	5.97	5.70	1.72
Z SD	0.25	0.94	0.80	0.78	0.12
Entropy	2.25	13.28	6.82	6.93	1.93
VAI	0.17	5.38	1.93	2.07	0.91

VCI	0.15	0.68	0.55	0.53	0.08
Mean crown area (m^2)	7.92	36.13	22.72	22.94	6.38
SD crown area	6.01	20.61	11.99	12.23	3.00
Foliar height diversity	0.68	3.10	2.50	2.43	0.39
25th percentile Z (m)	0.01	13.58	0.12	1.35	2.80
95th percentile Z (m)	6.71	34.58	18.45	18.97	4.58
LASCI	22.54	94.69	67.97	67.62	9.95
Field-derived metrics					
Trees/ha	200.77	6717.38	1491.89	1738.85	1156.13
Snags/ha	0.00	1842.64	95.49	201.22	303.94
BA/ha (m^2/ha)	5.19	70.27	34.77	35.20	9.58
Snag BA/ha (m^2/ha)	0.00	15.54	2.25	3.05	3.01
QMD (cm)	5.89	51.06	17.24	18.64	7.53
ASDI	222.96	3471.92	2168.65	2214.86	658.11
1 - (ASDI/SDI)	0.06	0.52	0.32	0.32	0.10
Trees/ha >40cm	0.00	68.79	19.04	21.69	16.68
DBH class H’	0.54	2.08	1.58	1.51	0.27
species H’	0.16	2.11	1.24	1.15	0.44
DBH class Gini coefficient	0.19	0.46	0.30	0.31	0.05
FASCI	41.90	74.18	65.51	64.18	6.83
ASCI	64.44	168.13	132.70	131.79	15.31
Point cloud density (points/m^2)	2.66	19.08	6.89	7.22	3.60

2.3.2 Principal components analysis

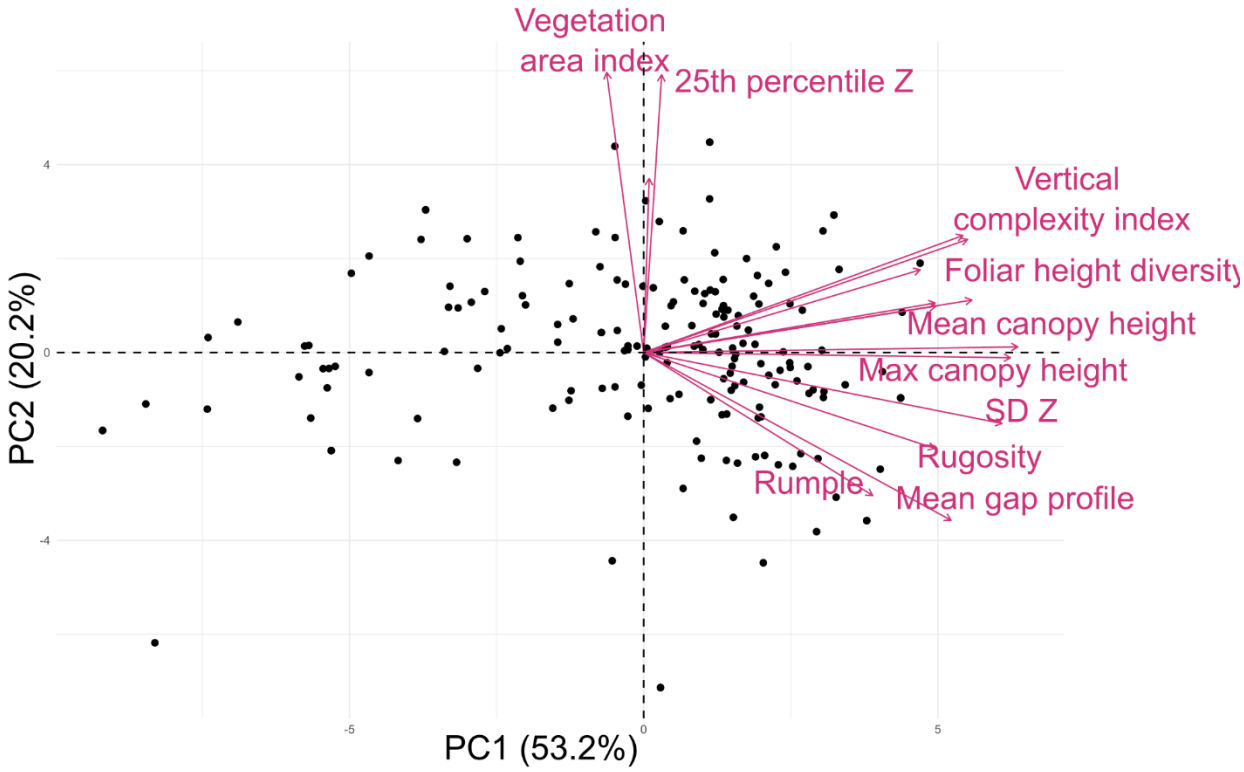

Figure 9 - Q1 lidar biplot.

The lidar-only PCAs showed similar patterns regarding the influence of chosen variables on the spatial arrangement. The vertical axis, PC2, has apparently strong, positive correlation with VAI and 25th percentile Z in both lidar-only PCAs. In the QL1 PCA (Figure 8), 73.4% of variation was explained by the first two axes, while in the QL2 PCA (Figure 9), 81.4% of the variation was explained by the first two axes.

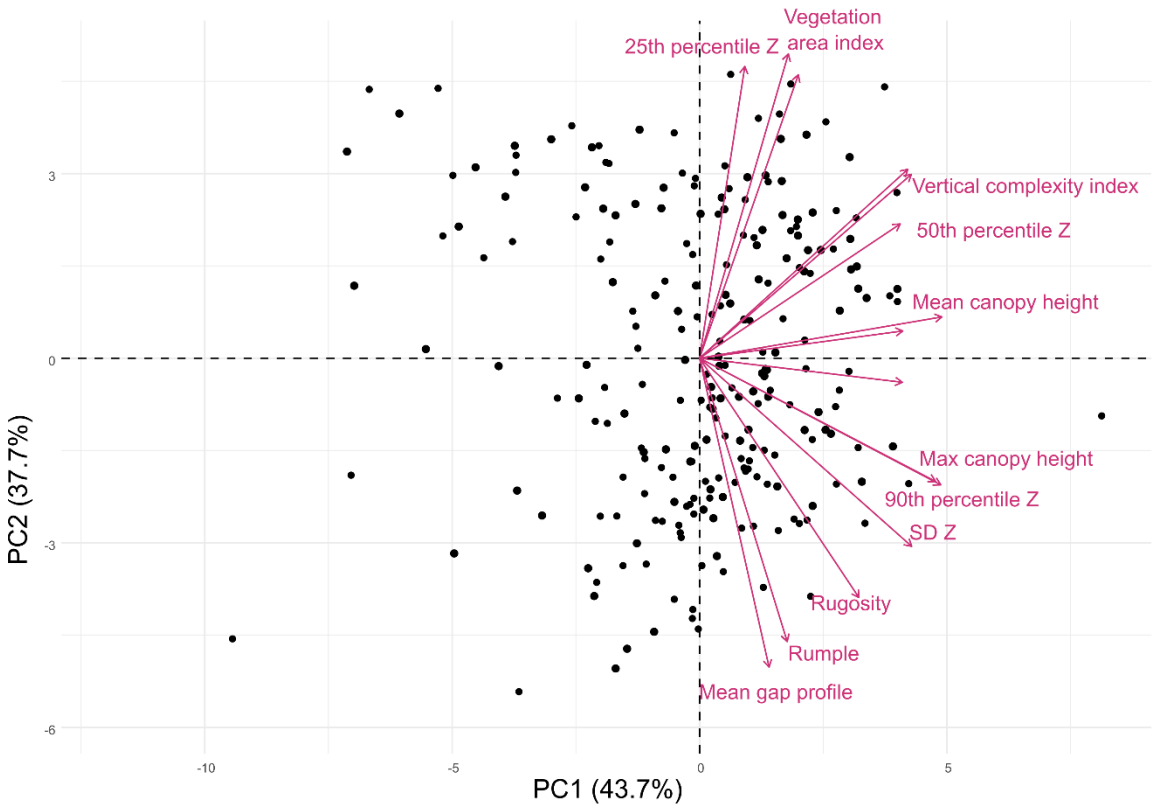

Figure 10 - QL2 lidar biplot

The top five variable contributions to PC1 (Figure 10) of the QL1 PCA were 95th percentile Z, maximum canopy height, standard deviation of Z, foliar height diversity and vertical complexity index. The top two variable contributions to PC2 of the QL1 PCA were vegetation area index and 25th percentile Z, both contributing over 20% of the variation displayed in PC2. The top five variable contributions to the QL2 PCA (Figure 11) were 95th percentile Z, maximum canopy height, standard deviation of Z, rugosity, and mean outer canopy height. The top three variable contributions to PC2 of the QL2 PCA were vegetation area index, entropy, and 25th percentile Z.

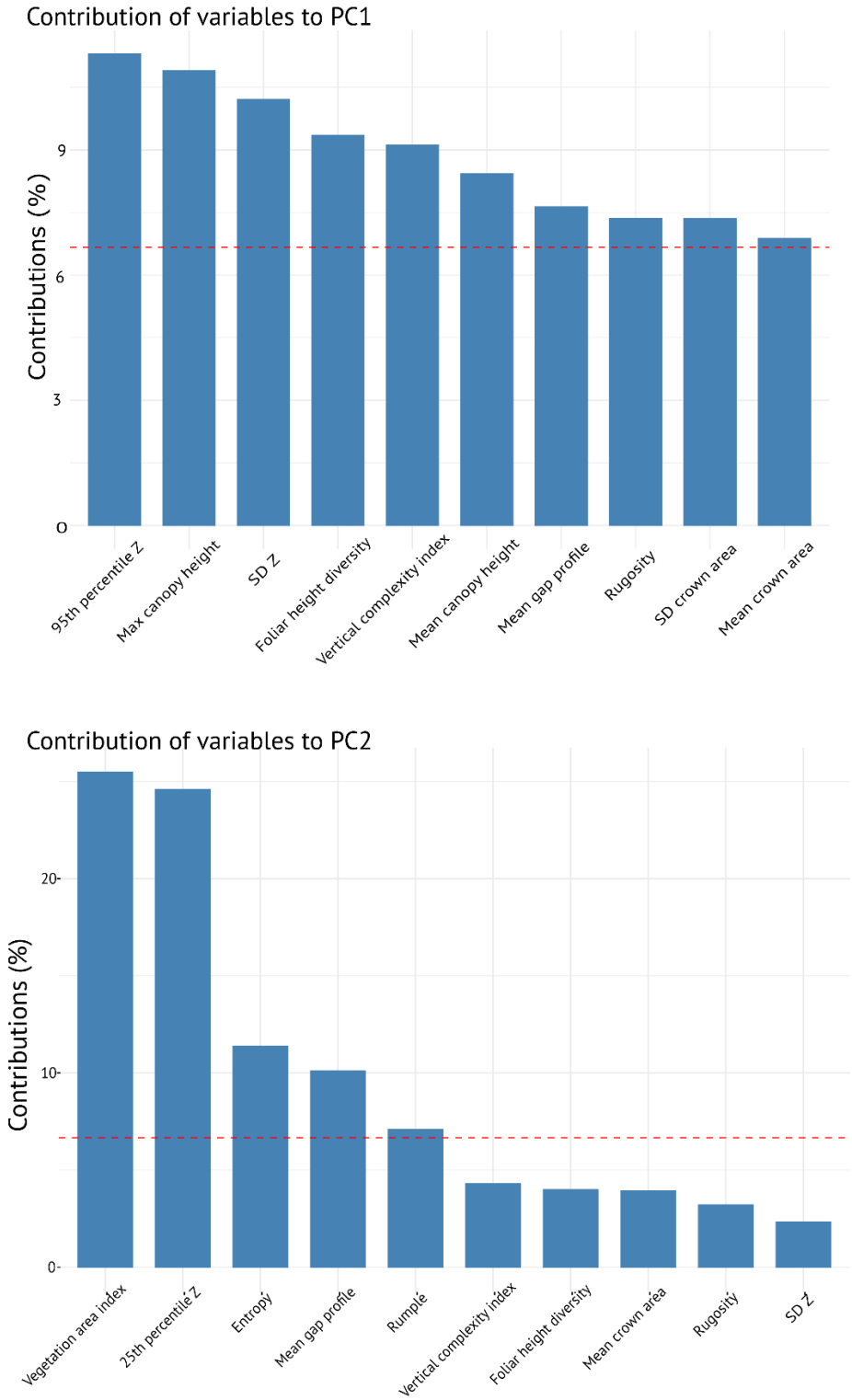

Figure 11 - QL1 lidar metrics PCA variable contributions. Top: contribution % of variables to PC1. Bottom: contributions of variables to PC2. The dashed red line marks the expected average contribution of a given variable.

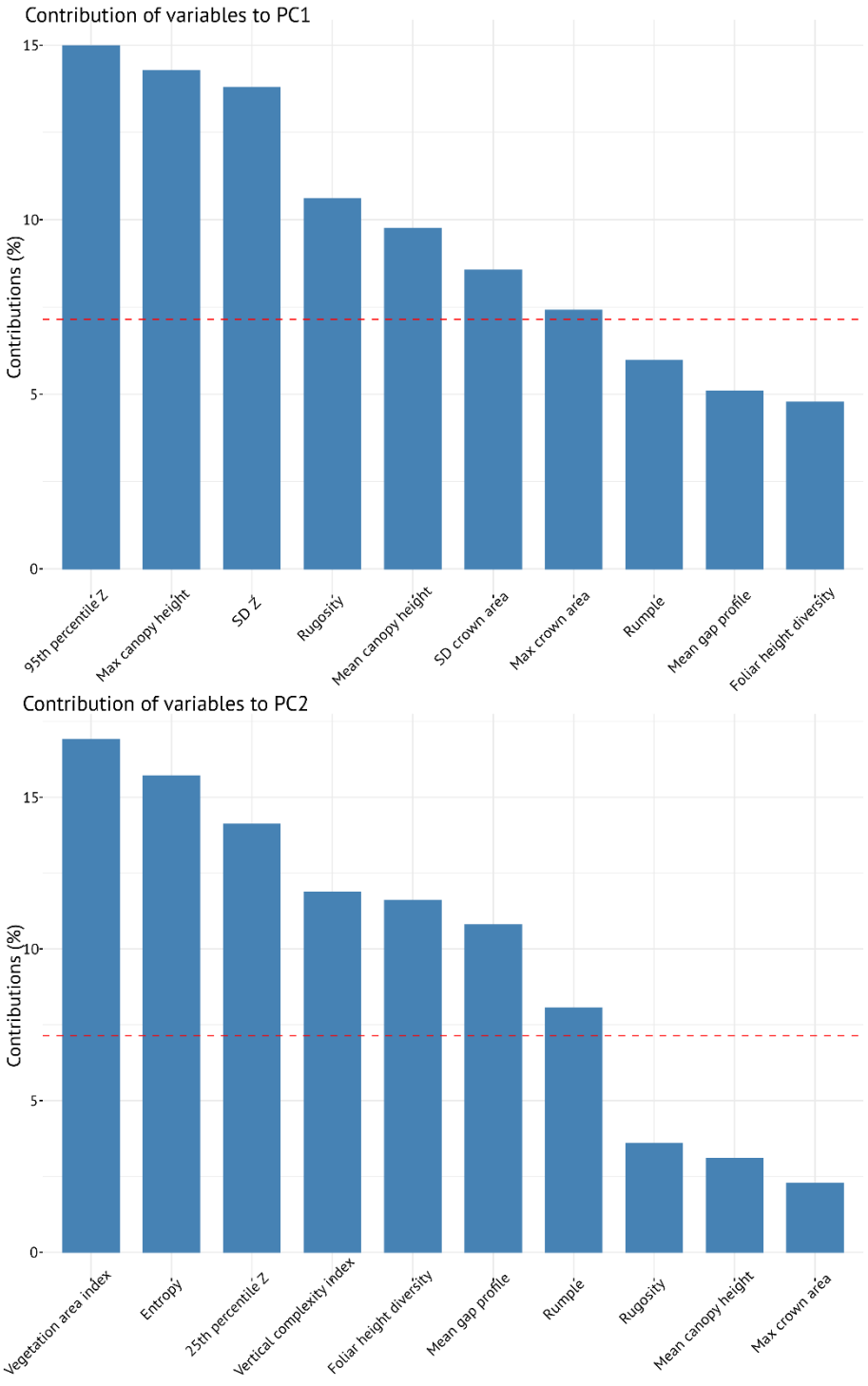

Figure 12 - QL2 lidar PCA variable contributions. Top: contributions of variables to PC1. Bottom: contribution of variables to PC2. The dashed red line marks the expected average contribution of a given variable.

In the PCA which includes the QL1 lidar data merged with field data (Figure 12), the first two axes explain 57.2% of the variation combined. In the PCA which includes the QL2 lidar data merged with field data (Figure 13), the first two axes explain 58.5% of the variation. In both merged biplots, similar patterns to the lidar-only PCAs are seen with some of the variables. 25th percentile and VAI appear to be positively correlated with the second axis. In the case of the lidar-only PCAs and the combined PCAs, the variation along the horizontal (first) axis seems to be related to size and height (e.g., mean outer canopy height, Shannon's index of DBH class, 95th percentile Z), while the variation along the vertical (second) axis seems to be more related to canopy closure or density (e.g., 25th percentile Z and VAI).

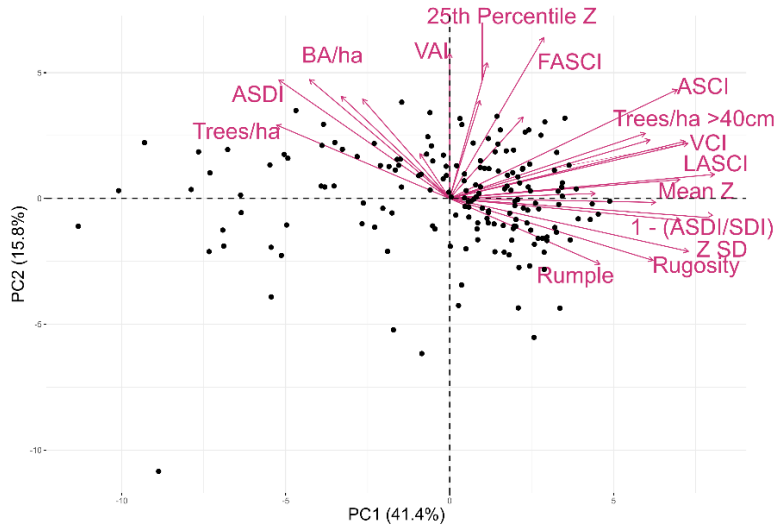

Figure 13 - PCA featuring QL1 lidar metrics merged with field-derived metrics. All plots sampled are within the WAMMO region.

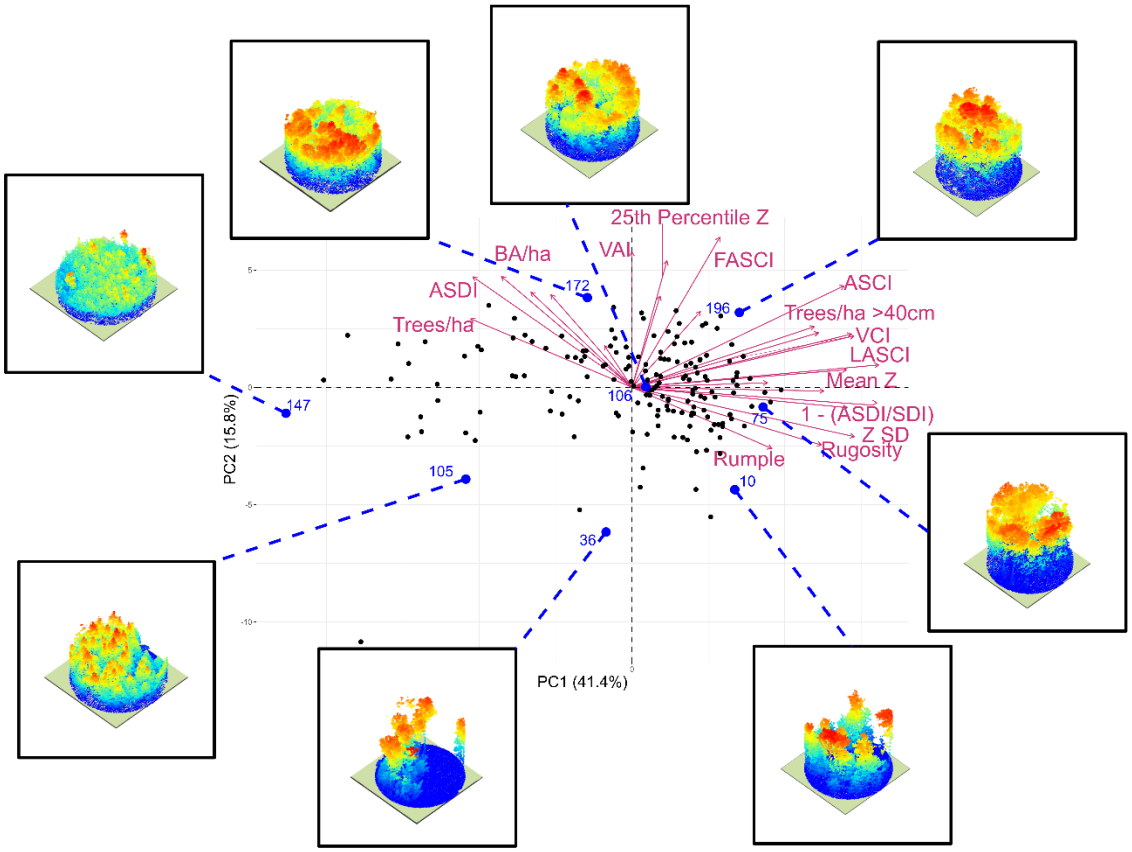

Figure 14 - PCA featuring QL1 lidar metrics merged with field-derived metrics along with lidar point clouds to visualize the forest structure represented by the biplot.

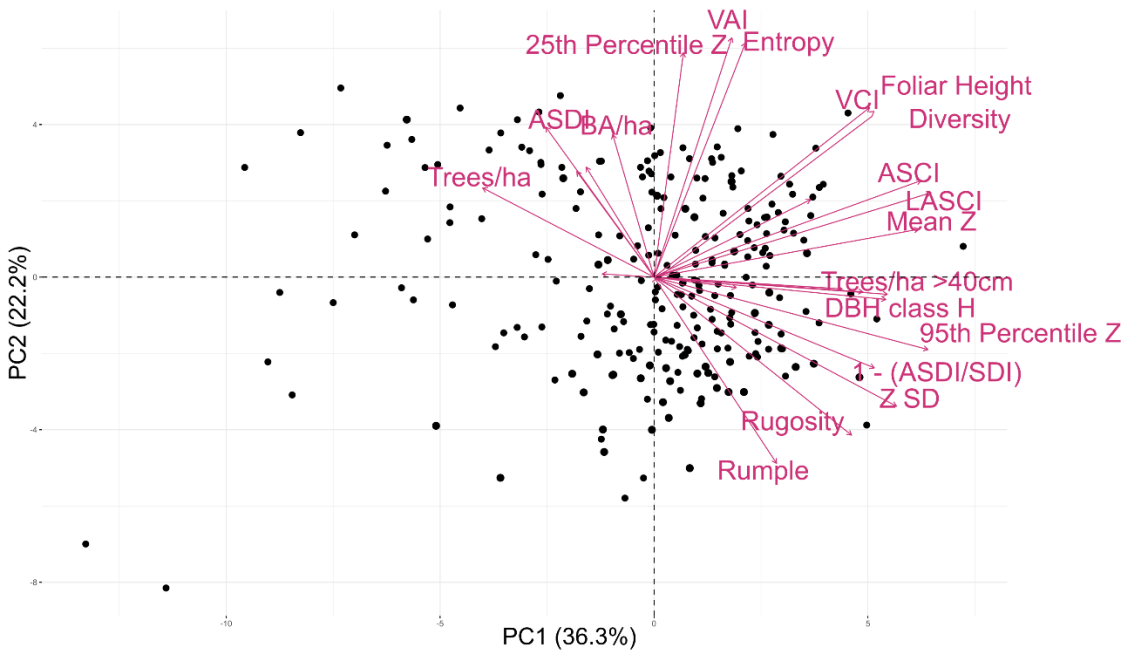

Figure 15 - PCA of QL2 lidar-derived metrics combined with field-derived metrics.

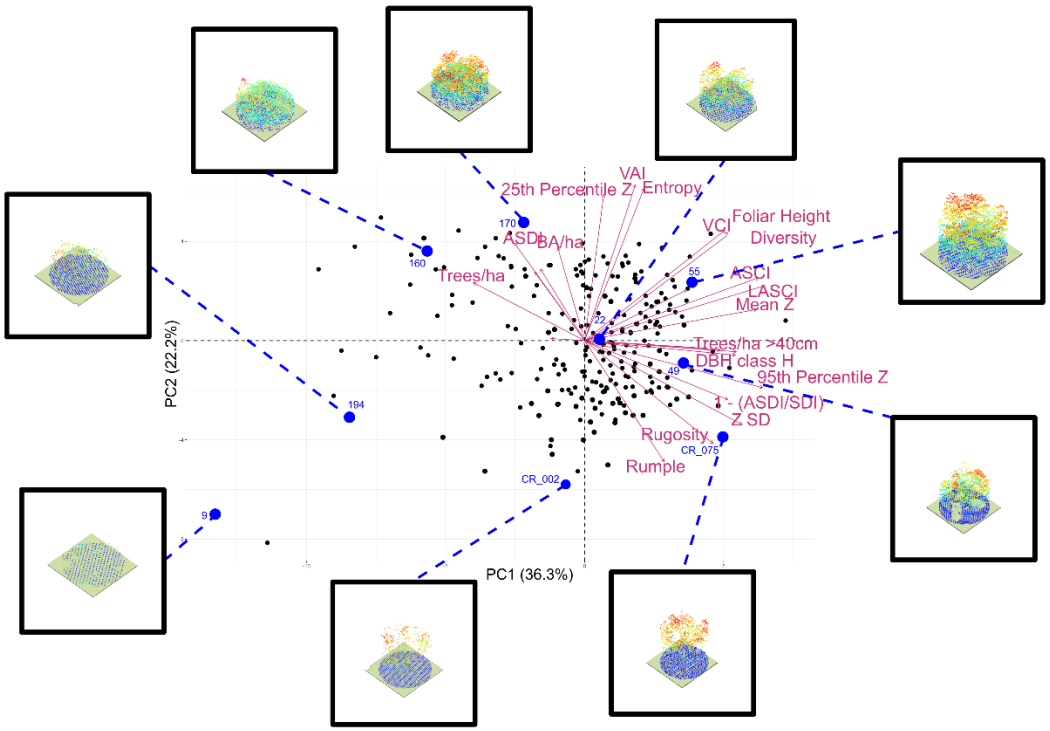

Figure 16 - PCA QL2 lidar-derived metrics combined with field-derived metrics with added lidar point clouds to visualize plots based on their placement in the PCA.

Of the selected field-derived metrics, three of them had strong correlations ($r > 0.6$) with QL2 lidar-derived metrics. The ratio of ASDI to SDI, large-diameter trees per hectare, and Shannon's index of DBH class all correlated positively with mean outer canopy height, standard deviation of Z and 95th percentile Z.

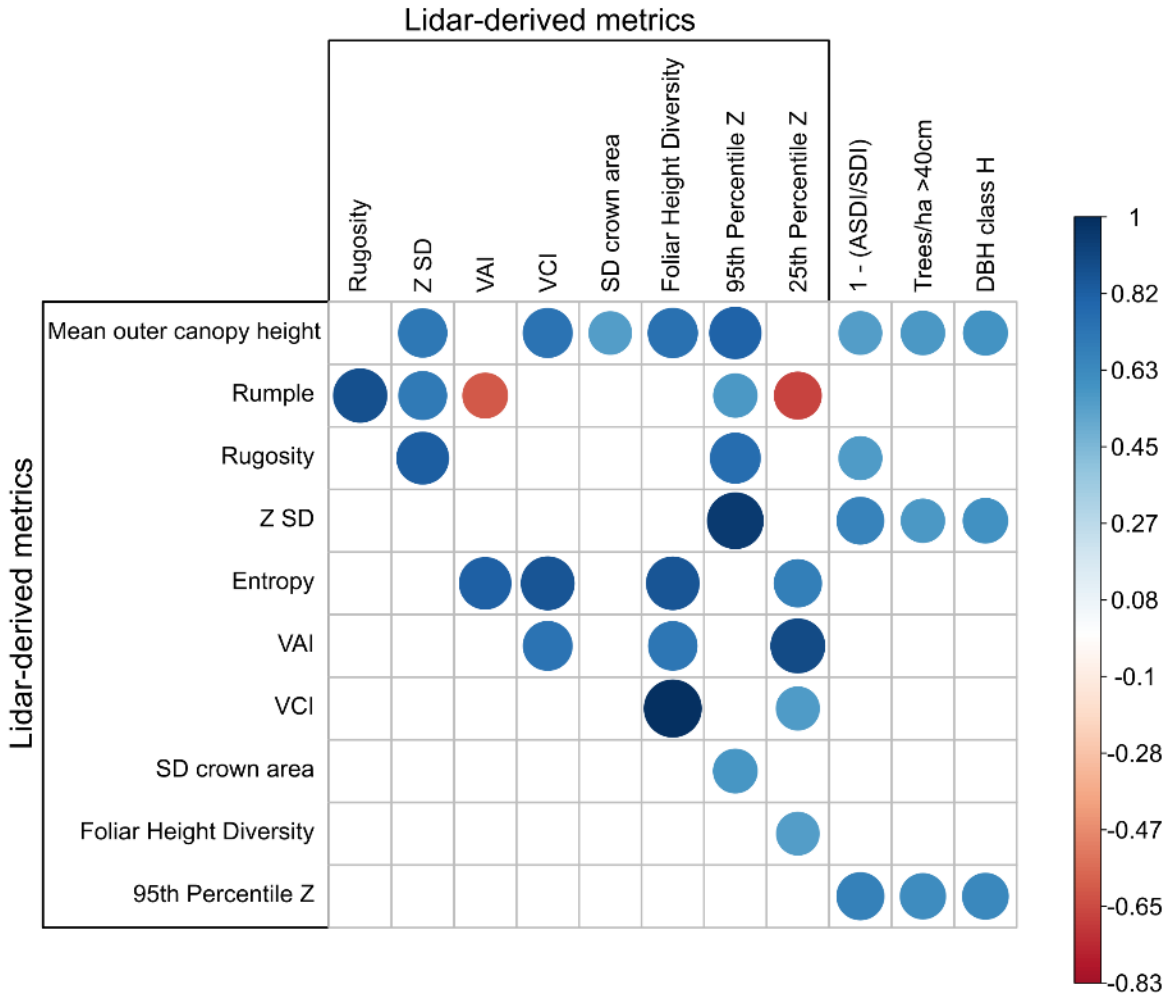

Figure 17 - selected QL2 variables and their correlations with one another and selected field-derived metrics. All correlations are significant to $p < 0.01$.

2.4 Discussion

Forest structural complexity (FSC) is an informative characteristic when it comes to sustainable forest management. It has been shown to be associated with ecosystem resilience, biodiversity, and carbon sequestration (Fahey et al., 2015; Hardiman et al., 2013; E. LaRue et al., 2019). This study assessed FSC metrics and their relationships by analyzing field measurements and lidar data side-by-side from common forest types in New Hampshire. These findings provide valuable insights into the understanding of measurements of FSC.

The principal components analysis (PCA) showed some important relationships between selected metrics. The first two axes on all PCAs explained a substantial portion of the variation exhibited by the plots. One trend worth noting is the types of variables that were associated with each of the first two axes. In all four PCAs performed in this study, the variables most associated with the first axis tended to be variables related to size (e.g., mean outer canopy height, 95th percentile Z, and Shannon's index of DBH class; i.e., vertical structure), while the variables most associated with the second axis tended to be variables related to canopy cover and density (e.g., 25th percentile Z and vegetation area index; i.e., horizontal structure). 25th percentile Z is more associated with canopy cover (i.e., horizontal structure) than higher percentile Z because, though trees between plots may be of similar height, if they are more densely spaced, the 25th percentile value will be higher because fewer lidar points reach the ground. This result is similar to what was found by Kane, McGaughey, et al. (2010), in a study of the relationship between field- and lidar-based metrics of forest structure.

Other studies have sought to understand the relationship between ground-based metrics, whether that is terrestrial lidar- (e.g., LaRue et al., 2020) or non-lidar-based (Kane, McGaughey, et al., 2010; Næsset, 2002) and aerial-based metrics of forest structure. Past studies have demonstrated the compatibility of aerial lidar-derived forest metrics and metrics derived from other sources. This study tends to find similar relationships between these metrics.

Three of the field-derived metrics displayed strong, positive correlations with lidar-derived metrics, namely Shannon's index of DBH class, the ratio of ASDI to SDI, and number of large-diameter trees per hectare. All of these metrics have been shown to have important implications for the complexity of stand structure (Ducey, 2009; Ducey & Larson, 2003; Long & Shaw, 2005; Lutz et al., 2018; Staudhammer & LeMay, 2001). Looking at the PCA, there is also an apparent similar contribution to the arrangement of plots between these three metrics and commonly-used lidar-derived metrics of structural complexity, like VCI, standard deviation of Z, rumple index, and rugosity. This indicates that perhaps these field-based metrics elucidate similar information about FSC as the lidar-derived metrics.

It is worth noting that quantifying FSC remains a challenging task due to the multitude of attributes and metrics involved. The ambiguity in defining complexity and interchangeability of terms such as diversity and heterogeneity can further complicate FSC assessments (Loke & Chisholm, 2022). Moreover, different metrics may reveal different aspects of forest structure, which is demonstrated by the contributions of the metrics used in this study. In the future, it would be useful to the field of study to establish more standardized definitions of FSC to ensure consistency and comparability across studies.

The combined PCA also revealed possible groupings of FSC variables, which can inform researchers on which variables to use when assessing FSC. The placement of variables within the PCA demonstrates their relatedness to one another, which, in this case, indicates which variables may be providing similar information. Based on these results, one could reasonably break the variables into 5 categories, drawing from field and lidar-derived metrics. These categories include **canopy height** (e.g., mean outer canopy height or 95th percentile Z), **height diversity** (e.g., foliar height diversity or vertical complexity index), **outer canopy complexity** (e.g., rumple index or rugosity), **canopy cover** (e.g., vegetation area index or 25th percentile Z), and **diameter diversity** (e.g., Shannon's index of DBH class or number of large trees per hectare). It is recommended that researchers who wish to assess FSC use one metric from each of those categories to obtain a detailed FSC assessment.

This study, of course, has some limitations. For one, this study only focused on forest types in New Hampshire, so some of these results should be replicated in other forest types. Because there can be considerable variation in the ways different forest types present structural complexity, it is possible that the results found here aren't completely generalizable. Further, this study relied on field-based measurements and aerial lidar-based measurements, but there are other data sources that could provide further insights into FSC like aerial imagery and terrestrial lidar.

In the future, it would be worthwhile to further explore these metrics in other contexts and with additional information. This study did not use information on stand age or land use history, and given the relationships between forest structure and stand age (Bradford &

Kastendick, 2010; Næsset, 2002), examining how it affects these FSC metrics would provide additional important information. Expanding the analysis to different regions and forest types can provide a more comprehensive understanding of FSC patterns and drivers. Furthermore, integrating multiple data sources, such as combining lidar data with aerial imagery or satellite data, can offer more detailed insights into forest structure dynamics.

CONCLUSIONS

Forest structural complexity holds significance for sustainable forest management and ecological understanding, with relationships to ecosystem resilience, biodiversity, and carbon sequestration (Fahey et al., 2015; Hardiman et al., 2013; E. LaRue et al., 2019). This study, encompassing New England mixed hardwood forests, aimed to decipher the impacts of spatial extent on FSC metrics, while examining the relationships between field measurements and lidar data.

The exploration into the influence of spatial extent on FSC metrics revealed high correlation values between FSC metrics obtained from smaller and larger plot sizes, raising the possibility of using smaller plots for effective representation of larger areas. Given the computational demands of processing lidar data, this finding could decrease the processing time required for lidar-derived metrics of FSC.

This study found possible groups of FSC metrics, which researchers can use for selecting metrics for assessments of FSC. These categories include **canopy height** (e.g., mean outer canopy height or 95th percentile Z), **height diversity** (e.g., foliar height diversity or vertical complexity index), **outer canopy complexity** (e.g., rumple index or rugosity), **canopy cover** (e.g., vegetation area index or 25th percentile Z), and **diameter diversity** (e.g., Shannon's index of DBH class or number of large trees per hectare). This offers an approach to comprehensively characterize FSC.

In conclusion, this study of FSC metrics in New England forests contributes valuable insights into the field of forest ecological research. These results can be helpful in the optimization of data processing efforts and the selection of FSC metrics. As ecological data

becomes more accessible, refining FSC assessment methodologies will be helpful to those who wish to characterize forest structure.

REFERENCES

Atkins, J., Bohrer, G., Fahey, R. T., Hardiman, B. S., Gough, C., Morin, T. H., Stovall, A. E. S., Stovall, A. E. L., & Zimmerman, N. (2020). *Ecosystem and Canopy Structural Complexity Metrics from LiDAR [R package forestr version 2.0.2]*.

Atkins, J., Bohrer, G., Fahey, R. T., Hardiman, B. S., Morin, T. H., Stovall, A. E. L., Zimmerman, N., & Gough, C. M. (2018). Quantifying vegetation and canopy structural complexity from terrestrial LiDAR data using the forestr r package. *Methods in Ecology and Evolution*, *9*(10), 2057–2066. https://doi.org/10.1111/2041-210x.13061

Atkins, J., Costanza, J., Dahlin, K. M., Dannenberg, M. P., Elmore, A. J., Fitzpatrick, M. C., Hakkenberg, C. R., Hardiman, B. S., Kamoske, A., LaRue, E. A., Silva, C. A., Stovall, A. E. L., & Tielens, E. K. (2023). Scale dependency of lidar-derived forest structural diversity. *Methods in Ecology and Evolution*, *14*(2), 708–723. https://doi.org/10.1111/2041-210X.14040

Atkins, J. W., Fahey, R. T., Hardiman, B. H., & Gough, C. M. (2018). Forest Canopy Structural Complexity and Light Absorption Relationships at the Subcontinental Scale. *Journal of Geophysical Research: Biogeosciences*, *123*(4), 1387–1405. https://doi.org/10.1002/2017JG004256

Bankston, J. B., Sabatia, C. O., & Poudel, K. P. (2021). Effects of Sample Plot Size and Prediction Models on Diameter Distribution Recovery. *Forest Science*, *67*(3), 245–255. https://doi.org/10.1093/forsci/fxaa055

Bradford, J. B., & Kastendick, D. N. (2010). Age-related patterns of forest complexity and carbon storage in pine and aspen–birch ecosystems of northern Minnesota, USA.

Canadian Journal of Forest Research, *40*(3), 401–409. https://doi.org/10.1139/X10-002

Bravo, F., del Río, M., Bravo-Oviedo, A., Del Peso, C., Montero, G., & Montero, G. (2008). *Forest Management Strategies and Carbon Sequestration*. 179–194. https://doi.org/10.1007/978-1-4020-8343-3_11

Buongiorno, J. (2001). Quantifying the implications of transformation from even to uneven-aged forest stands. *Forest Ecology and Management*, *151*(1–3), 121–132. https://doi.org/10.1016/S0378-1127(00)00702-7

Chungan Li, Xin Lin, Huabing Dai, Zhen Li, & Mei Zhou. (2022). Effects of Plot Size on Airborne LiDAR-Derived Metrics and Predicted Model Performances of Subtropical Planted Forest Attributes. *Forests*. https://doi.org/10.3390/f13122124

Colter, R. A. (2019). *ADVANCING THE TERRESTRIAL ECOLOGICAL UNIT INVENTORY WITHIN THE WHITE MOUNTAIN NATIONAL FOREST USING LiDAR*.

Côté, J.-F., Widlowski, J.-L., Fournier, R. A., & Verstraete, M. M. (2009). The structural and radiative consistency of three-dimensional tree reconstructions from terrestrial lidar. *Remote Sensing of Environment*, *113*(5), 1067–1081. https://doi.org/10.1016/j.rse.2009.01.017

Danson, F. M., Hetherington, D., Morsdorf, F., Koetz, B., & Allgower, B. (2007). Forest Canopy Gap Fraction From Terrestrial Laser Scanning. *IEEE Geoscience and Remote Sensing Letters*, *4*(1), 157–160. https://doi.org/10.1109/LGRS.2006.887064

Dasgupta, P., Sen, A., & Starrett, D. (1973). Notes on the measurement of inequality. *Journal of Economic Theory*, *6*(2), 180–187. https://doi.org/10.1016/0022-0531(73)90033-1

Deo, R. K., Froese, R. E., Falkowski, M. J., & Hudak, A. T. (2016). Optimizing Variable Radius Plot Size and LiDAR Resolution to Model Standing Volume in Conifer Forests. *Canadian Journal of Remote Sensing*, *42*(5), 428–442. https://doi.org/10.1080/07038992.2016.1220826

DeWalt, S. J., Maliakal, S. K., & Denslow, J. S. (2003). Changes in vegetation structure and composition along a tropical forest chronosequence: Implications for wildlife. *Forest Ecology and Management*, *182*(1–3), 139–151. https://doi.org/10.1016/S0378-1127(03)00029-X

Ducey, M. J. (2009). The Ratio of Additive and Traditional Stand Density Indices. *Western Journal of Applied Forestry*, *24*(1), 5–10. https://doi.org/10.1093/wjaf/24.1.5

Ducey, M. J., & Larson, B. C. (2003). Is There a Correct Stand Density Index? An Alternate Interpretation. *Western Journal of Applied Forestry*, *18*(3), 179–184. https://doi.org/10.1093/wjaf/18.3.179

Fahey, R. T., Alveshere, B. C., Burton, J. I., D'Amato, A. W., Dickinson, Y. L., Keeton, W. S., Kern, C. C., Larson, A. J., Palik, B. J., Puettmann, K. J., Saunders, M. R., Webster, C. R., Atkins, J. W., Gough, C. M., & Hardiman, B. S. (2018). Shifting conceptions of complexity in forest management and silviculture. *Forest Ecology and Management*, *421*, 59–71. https://doi.org/10.1016/j.foreco.2018.01.011

Fahey, R. T., Fotis, A. T., & Woods, K. D. (2015). Quantifying canopy complexity and effects on productivity and resilience in late-successional hemlock–hardwood forests. *Ecological Applications*, *25*(3), 834–847. https://doi.org/10.1890/14-1012.1

Franklin, J. F., Cromack, K., Denison, W., McKee, A., Maser, C., Sedell, J. R., Swanson, F., & Juday, Glen. (1981). *Ecological Characteristics of Old-Growth Douglas-Fir Forests*. https://doi.org/10.2737/pnw-gtr-118

Franklin, J. F., & Spies, T. A. (n.d.). Composition, Function, and Structure of Old-Growth Douglas-Fir Forests. *Wildlife and Vegetation of Unmanaged Douglas-Fir Forests. USDA Forest Service, Portland, Oregon*, 91–109.

Franklin, J. F., Spies, T. A., Pelt, R. V., Carey, A. B., Thornburgh, D. A., Berg, D. R., Lindenmayer, D. B., Harmon, M. E., Keeton, W. S., Shaw, D. C., Bible, K., & Chen, J. (2002). Disturbances and structural development of natural forest ecosystems with silvicultural implications, using Douglas-fir forests as an example. *Forest Ecology and Management*, *155*(1–3), 399–423. https://doi.org/10.1016/S0378-1127(01)00575-8

Frazer, G. W., Magnussen, S., Wulder, M. A., & Niemann, K. O. (2011). Simulated impact of sample plot size and co-registration error on the accuracy and uncertainty of LiDAR-derived estimates of forest stand biomass. *Remote Sensing of Environment*, *115*(2), 636–649. https://doi.org/10.1016/j.rse.2010.10.008

Gibbons, P., Lindenmayer, D. B., Barry, S. C., & Tanton, M. T. (2002). Hollow selection by vertebrate fauna in forests of southeastern Australia and implications for forest management. *Biological Conservation*, *103*(1), 1–12. https://doi.org/10.1016/S0006-3207(01)00109-4

Gobakken, T., Erik Næsset, & Næsset, E. (2008). Assessing effects of laser point density, ground sampling intensity, and field sample plot size on biophysical stand

properties derived from airborne laser scanner data. *Canadian Journal of Forest Research*, *38*(5), 1095–1109. https://doi.org/10.1139/x07-219

Gough, C. M., Atkins, J. W., Fahey, R. T., & Hardiman, B. S. (2019). High rates of primary production in structurally complex forests. *Ecology*, *100*(10). https://doi.org/10.1002/ecy.2864

Gough, C. M., Curtis, P. S., Hardiman, B. S., Scheuermann, C. M., & Bond-Lamberty, B. (2016). Disturbance, complexity, and succession of net ecosystem production in North America's temperate deciduous forests. *Ecosphere*, *7*(6). https://doi.org/10.1002/ecs2.1375

Gunn, J. S., Ducey, M. J., & Whitman, A. A. (2014). Late-successional and old-growth forest carbon temporal dynamics in the Northern Forest (Northeastern USA). *Forest Ecology and Management*, *312*, 40–46. https://doi.org/10.1016/j.foreco.2013.10.023

Hardiman, B. S., Bohrer, G., Gough, C. M., Vogel, C. S., & Curtis, P. S. (2011). The role of canopy structural complexity in wood net primary production of a maturing northern deciduous forest. *Ecology*, *92*(9), 1818–1827. https://doi.org/10.1890/10-2192.1

Hardiman, B. S., Gough, C. M., Halperin, A., Hofmeister, K. L., Nave, L. E., Bohrer, G., & Curtis, P. S. (2013). Maintaining high rates of carbon storage in old forests: A mechanism linking canopy structure to forest function. *Forest Ecology and Management*, *298*, 111–119. https://doi.org/10.1016/j.foreco.2013.02.031

Hayashi, R., Weiskittel, A. R., & Sader, S. A. (2014). Assessing the Feasibility of Low-Density LiDAR for Stand Inventory Attribute Predictions in Complex and Managed Forests of Northern Maine, USA. *Forests*, *5*(2), 363–383. https://doi.org/10.3390/f5020363

Hilker, T., Coops, N. C., Newnham, G. J., van Leeuwen, M., Wulder, M. A., Stewart, J., & Culvenor, D. S. (2012). Comparison of Terrestrial and Airborne LiDAR in Describing Stand Structure of a Thinned Lodgepole Pine Forest. *Journal of Forestry*, *110*(2), 97–104. https://doi.org/10.5849/jof.11-003

Homeier, J., Breckle, S.-W., Günter, S., Rollenbeck, R. T., & Leuschner, C. (2010). Tree Diversity, Forest Structure and Productivity along Altitudinal and Topographical Gradients in a Species-Rich Ecuadorian Montane Rain Forest: Ecuadorian Montane Forest Diversity and Structure. *Biotropica*, *42*(2), 140–148. https://doi.org/10.1111/j.1744-7429.2009.00547.x

Hooper, D. U., Chapin, F. S., Ewel, J. J., Hector, A., Inchausti, P., Lavorel, S., Lawton, J. H., Lodge, D. M., Loreau, M., Naeem, S., Schmid, B., Setälä, H., Symstad, A. J., Vandermeer, J., & Wardle, D. A. (2005). EFFECTS OF BIODIVERSITY ON ECOSYSTEM FUNCTIONING: A CONSENSUS OF CURRENT KNOWLEDGE. *Ecological Monographs*, *75*(1), 3–35. https://doi.org/10.1890/04-0922

Hummel, S., Hudak, A. T., Uebler, E. H., Falkowski, M. J., & Megown, K. A. (2011). A Comparison of Accuracy and Cost of LiDAR versus Stand Exam Data for Landscape Management on the Malheur National Forest. *Journal of Forestry*, *109*(5), 267–273. https://doi.org/10.1093/jof/109.5.267

Jackson, H. B., & Fahrig, L. (2015). Are ecologists conducting research at the optimal scale? *Global Ecology and Biogeography*, *24*(1), 52–63. https://doi.org/10.1111/geb.12233

Jeong, N., Hwang, H., & Matson, E. T. (2018). Evaluation of low-cost LiDAR sensor for application in indoor UAV navigation. *2018 IEEE Sensors Applications Symposium (SAS)*, 1–5. https://doi.org/10.1109/SAS.2018.8336719

Johnson, D. W., & Curtis, P. S. (2001). Effects of forest management on soil C and N storage: Meta analysis. *Forest Ecology and Management*, *140*(2–3), 227–238. https://doi.org/10.1016/S0378-1127(00)00282-6

Jung, K., Kaiser, S., Böhm, S., Nieschulze, J., & Kalko, E. K. V. (2012). Moving in three dimensions: Effects of structural complexity on occurrence and activity of insectivorous bats in managed forest stands: *Bats and 3D forest structure*. *Journal of Applied Ecology*, *49*(2), 523–531. https://doi.org/10.1111/j.1365-2664.2012.02116.x

Kane, V. R., Bakker, J. D., McGaughey, R. J., Lutz, J. A., Gersonde, R. F., & Franklin, J. F. (2010). Examining conifer canopy structural complexity across forest ages and elevations with LiDAR data. *Canadian Journal of Forest Research*, *40*(4), 774–787. https://doi.org/10.1139/X10-064

Kane, V. R., McGaughey, R. J., Bakker, J. D., Gersonde, R. F., Lutz, J. A., & Franklin, J. F. (2010). Comparisons between field- and LiDAR-based measures of stand structural complexity. *Canadian Journal of Forest Research*, *40*(4), 761–773. https://doi.org/10.1139/X10-024

Kassambara, A., & Mundt, F. (2020). *factoextra: Extract and Visualize the Results of Multivariate Data Analyses* (1.0.7) [Computer software]. https://CRAN.R-project.org/package=factoextra

Lal, R. (2005). Forest soils and carbon sequestration. *Forest Ecology and Management*, *220*(1–3), 242–258. https://doi.org/10.1016/j.foreco.2005.08.015

LaRue, E. A., Fahey, R., Fuson, T. L., Foster, J. R., Matthes, J. H., Krause, K., & Hardiman, B. S. (2022). Evaluating the sensitivity of forest structural diversity characterization to LiDAR point density. *Ecosphere*, *13*(9). https://doi.org/10.1002/ecs2.4209

LaRue, E., Hardiman, B. S., Elliott, J. M., & Fei, S. (2019). Structural diversity as a predictor of ecosystem function. *Environmental Research Letters*, *14*(11), 114011. https://doi.org/10.1088/1748-9326/ab49bb

LaRue, E., Wagner, F., Fei, S., Atkins, J., Fahey, R., Gough, C., & Hardiman, B. (2020). Compatibility of Aerial and Terrestrial LiDAR for Quantifying Forest Structural Diversity. *Remote Sensing*, *12*(9), 1407. https://doi.org/10.3390/rs12091407

Le, S., Josse, J., & Husson, F. (2008). FactoMineR: An R Package for Multivariate Analysis. *Journal of Statistical Software*, *25*(1), 1–18. https://doi.org/10.18637/jss.v025.i01

Lefsky, M. A., Cohen, W. B., Acker, S. A., Parker, G. G., Spies, T. A., & Harding, D. (1999). Lidar Remote Sensing of the Canopy Structure and Biophysical Properties of Douglas-Fir Western Hemlock Forests. *Remote Sensing of Environment*, *70*(3), 339–361. https://doi.org/10.1016/S0034-4257(99)00052-8

Levin, S. A. (1992). The Problem of Pattern and Scale in Ecology: The Robert H. MacArthur Award Lecture. *Ecology*, *73*(6), 1943–1967. https://doi.org/10.2307/1941447

Lexerød, N. L., & Eid, T. (2006). An evaluation of different diameter diversity indices based on criteria related to forest management planning. *Forest Ecology and Management*, *222*(1–3), 17–28. https://doi.org/10.1016/j.foreco.2005.10.046

Li, H., & Reynolds, J. F. (1995). On Definition and Quantification of Heterogeneity. *Oikos*, *73*(2), 280. https://doi.org/10.2307/3545921

Lim, K., Treitz, P., Wulder, M. A., St-Onge, B., & Flood, M. (2003). LiDAR remote sensing of forest structure. *Progress in Physical Geography*, *27*(1), 88–106. https://doi.org/10.1191/0309133303pp360ra

Lindenmayer, D. B. (2019). Integrating forest biodiversity conservation and restoration ecology principles to recover natural forest ecosystems. *New Forests*, *50*(2), 169–181. https://doi.org/10.1007/s11056-018-9633-9

Lindenmayer, D. B., Margules, C. R., & Botkin, D. B. (2000). Indicators of Biodiversity for Ecologically Sustainable Forest Management. *Conservation Biology*, *14*(4), 941–950. https://doi.org/10.1046/j.1523-1739.2000.98533.x

Loke, L. H. L., & Chisholm, R. A. (2022). Measuring habitat complexity and spatial heterogeneity in ecology. *Ecology Letters*, ele.14084. https://doi.org/10.1111/ele.14084

Long, J. N., & Shaw, J. D. (2005). A Density Management Diagram for Even-aged Ponderosa Pine Stands. *Western Journal of Applied Forestry*, *20*(4), 205–215. https://doi.org/10.1093/wjaf/20.4.205

Lutz, J. A., Furniss, T. J., Johnson, D. J., Davies, S. J., Allen, D., Alonso, A., Anderson-Teixeira, K. J., Andrade, A., Baltzer, J., Becker, K. M. L., Blomdahl, E. M., Bourg, N. A., Bunyavejchewin, S., Burslem, D. F. R. P., Cansler, C. A., Cao, K., Cao, M., Cardenas, D., Chang, L.-W., … Zimmerman, J. K. (2018). Global importance of large-diameter trees. *Global Ecology and Biogeography*, *27*(7), 849–864. https://doi.org/10.1111/geb.12747

MacArthur, R. H., & Horn, H. S. (1969). Foliage Profile by Vertical Measurements. *Ecology*, *50*(5), 802–804. https://doi.org/10.2307/1933693

MacArthur, R. H., & MacArthur, J. W. (1961). On Bird Species Diversity. *Ecology*, *42*(3), 594–598. https://doi.org/10.2307/1932254

MacArthur, R., Recher, H., & Cody, M. (1966). On the Relation between Habitat Selection and Species Diversity. *The American Naturalist*, *100*(913), 319–332. https://doi.org/10.1086/282425

Magurran, A. E. (1988). *Diversity indices and species abundance models*. 7–45. https://doi.org/10.1007/978-94-015-7358-0_2

McElhinny, C., Gibbons, P., Brack, C., & Bauhus, J. (2005). Forest and woodland stand structural complexity: Its definition and measurement. *Forest Ecology and Management*, *218*(1–3), 1–24. https://doi.org/10.1016/j.foreco.2005.08.034

McNab, W. H., Cleland, D. T., Freeouf, J. A., Keys, J. E., Nowacki, G. J., & Carpenter, C. A. (2007). *Description of ecological subregions: Sections of the conterminous United States* (WO-GTR-76B; p. WO-GTR-76B). U.S. Department of Agriculture, Forest Service. https://doi.org/10.2737/WO-GTR-76B

Means, J. E., Acker, S. A., Renslow, M., Emerson, L., & Hendrix, C. J. (2000). Predicting Forest Stand Characteristics with Airborne Scanning Lidar. *PHOTOGRAMMETRIC ENGINEERING*, *66*(11), 1367–1371.

Murphy, B. A., May, J. A., Butterworth, B. J., Andresen, C. G., & Desai, A. R. (2022). Unraveling Forest Complexity: Resource Use Efficiency, Disturbance, and the Structure-Function Relationship. *Journal of Geophysical Research: Biogeosciences*, *127*(6). https://doi.org/10.1029/2021JG006748

Næsset, E. (2002). Predicting forest stand characteristics with airborne scanning laser using a practical two-stage procedure and field data. *Remote Sensing of Environment*, *80*(1), 88–99. https://doi.org/10.1016/S0034-4257(01)00290-5

Nagy, R. C., Balch, J. K., Bissell, E. K., Cattau, M. E., Glenn, N. F., Halpern, B. S., Ilangakoon, N., Johnson, B., Joseph, M. B., Marconi, S., O'Riordan, C., Sanovia, J., Swetnam, T. L., Travis, W. R., Wasser, L. A., Woolner, E., Zarnetske, P., Abdulrahim, M., Adler, J., … Zhu, K. (2021). Harnessing the NEON data revolution to advance open environmental science with a diverse and data-capable community. *Ecosphere*, *12*(12). https://doi.org/10.1002/ecs2.3833

Nelson, R., Krabill, W., & MacLean, G. (1984). Determining forest canopy characteristics using airborne laser data. *Remote Sensing of Environment*, *15*(3), 201–212. https://doi.org/10.1016/0034-4257(84)90031-2

Noss, R. F. (1990). Indicators for Monitoring Biodiversity: A Hierarchical Approach. *Conservation Biology*, *4*(4), 355–364. https://doi.org/10.1111/j.1523-1739.1990.tb00309.x

Nunery, J. S., & Keeton, W. S. (2010). Forest carbon storage in the northeastern United States: Net effects of harvesting frequency, post-harvest retention, and wood products. *Forest Ecology and Management*, *259*(8), 1363–1375. https://doi.org/10.1016/j.foreco.2009.12.029

Pommerening, A. (2002). Approaches to quantifying forest structures. *Forestry*, *75*(3), 305–324. https://doi.org/10.1093/forestry/75.3.305

Puettmann, K. J., & Messier, C. (2019). Simple Guidelines to Prepare Forests for Global Change: The Dog and the Frisbee. *Northwest Science*, *93*(3–4), 209. https://doi.org/10.3955/046.093.0305

Qi, Y., & Wu, J. (1996). Effects of changing spatial resolution on the results of landscape pattern analysis using spatial autocorrelation indices. *Landscape Ecology*, *11*(1), 39–49. https://doi.org/10.1007/bf02087112

R Core Team. (2022). *R: A language and environment for statistical computing* [Computer software]. R Foundation for Statistical Computing. https://www.R-project.org/

Roussel, J.-R., documentation), D. A. (Reviews the, features), F. D. B. (Fixed bugs and improved catalog, segment_snags()), A. S. M. (Implemented wing2015() for, track_sensor()), B. J.-F. (Contributed to R. for, track_sensor()), G. D. (Implemented G. for, management), L. S. (Contributed to parallelization, & code), S. A. (Author of the C. concaveman. (2023). *lidR: Airborne LiDAR Data Manipulation and Visualization for Forestry Applications* (4.0.3) [Computer software]. https://cran.r-project.org/web/packages/lidR/index.html

Sarkar, S. (2002). Defining "Biodiversity"; Assessing Biodiversity. *The Monist*, *85*(1), 131–155. https://doi.org/10.5840/monist20028515

Schulte, B. J., & Buongiorno, J. (1998). Effects of uneven-aged silviculture on the stand structure, species composition, and economic returns of loblolly pine stands. *Forest Ecology and Management*, *111*(1), 83–101. https://doi.org/10.1016/S0378-1127(98)00312-0

Signorell, A. (2022). *DescTools: Tools for descriptive statistics* (0.99.47) [Computer software].

Simpson, E. H. (1949). Measurement of diversity. *Nature*, *163*(4148), 688–688. https://doi.org/10.1038/163688a0

Staudhammer, C. L., & LeMay, V. M. (2001). Introduction and evaluation of possible indices of stand structural diversity. *Canadian Journal of Forest Research*, *31*(7), 1105–1115. https://doi.org/10.1139/x01-033

Stein, A., Gerstner, K., & Kreft, H. (2014). Environmental heterogeneity as a universal driver of species richness across taxa, biomes and spatial scales. *Ecology Letters*, *17*(7), 866–880. https://doi.org/10.1111/ele.12277

Takacs, D. (1996). *The Idea of Biodiversity: Philosophies of Paradise*.

Taylor, S. L., & MacLean, D. A. (2009). Legacy of Insect Defoliators: Increased Wind-Related Mortality Two Decades After a Spruce Budworm Outbreak. *Forest Science*, *55*(3), 256–267.

Tews, J., Brose, U., Grimm, V., Tielbörger, K., Wichmann, M. C., Schwager, M., & Jeltsch, F. (2004). Animal species diversity driven by habitat heterogeneity/diversity: The importance of keystone structures: Animal species diversity driven by habitat heterogeneity. *Journal of Biogeography*, *31*(1), 79–92. https://doi.org/10.1046/j.0305-0270.2003.00994.x

Thom, D., & Keeton, W. S. (2019). Stand structure drives disparities in carbon storage in northern hardwood-conifer forests. *Forest Ecology and Management*, *442*, 10–20. https://doi.org/10.1016/j.foreco.2019.03.053

Valbuena, R., Packalén, P., Martı´n-Fernández, S., & Maltamo, M. (2012). Diversity and equitability ordering profiles applied to study forest structure. *Forest Ecology and Management*, *276*, 185–195. https://doi.org/10.1016/j.foreco.2012.03.036

Watt, P. J., & Donoghue, D. N. M. (2005). Measuring forest structure with terrestrial laser scanning. *International Journal of Remote Sensing*, *26*(7), 1437–1446. https://doi.org/10.1080/01431160512331337961

Weiner, J., & Solbrig, O. T. (1984). The meaning and measurement of size hierarchies in plant populations. *Oecologia*, *61*(3), 334–336. https://doi.org/10.1007/BF00379630

Whittaker, R. H. (1972). Evolution and measurement of species diversity. *Taxon*, *21*(2), 213–251. https://doi.org/10.2307/1218190

Wiens, J. A. (1989). Spatial Scaling in Ecology. *Functional Ecology*, *3*(4), 385. https://doi.org/10.2307/2389612

Wood, E. F., Sivapalan, M., & Beven, K. (1990). Similarity and scale in catchment storm response. *Reviews of Geophysics*, *28*(1), 1. https://doi.org/10.1029/RG028i001p00001

Wood, E. F., Sivapalan, M., Beven, K., & Band, L. (1988). Effects of spatial variability and scale with implications to hydrologic modeling. *Journal of Hydrology*, *102*(1–4), 29–47. https://doi.org/10.1016/0022-1694(88)90090-X

Wu, J. (1999). Hierarchy and scaling: Extrapolating information along a scaling ladder. *Canadian Journal of Remote Sensing*, *25*(4), 367–380. https://doi.org/10.1080/07038992.1999.10874736

Wu, J. (2004). Effects of changing scale on landscape pattern analysis: Scaling relations. *Landscape Ecology*, *19*(2), 125–138. https://doi.org/10.1023/B:LAND.0000021711.40074.ae

Zenner, E. K. (2004). Does old-growth condition imply high live-tree structural complexity? *Forest Ecology and Management*, *195*(1–2), 243–258. https://doi.org/10.1016/j.foreco.2004.03.026

Zenner, E. K., & Hibbs, D. E. (2000). A new method for modeling the heterogeneity of forest structure. *Forest Ecology and Management*, *129*(1–3), 75–87. https://doi.org/10.1016/S0378-1127(99)00140-1